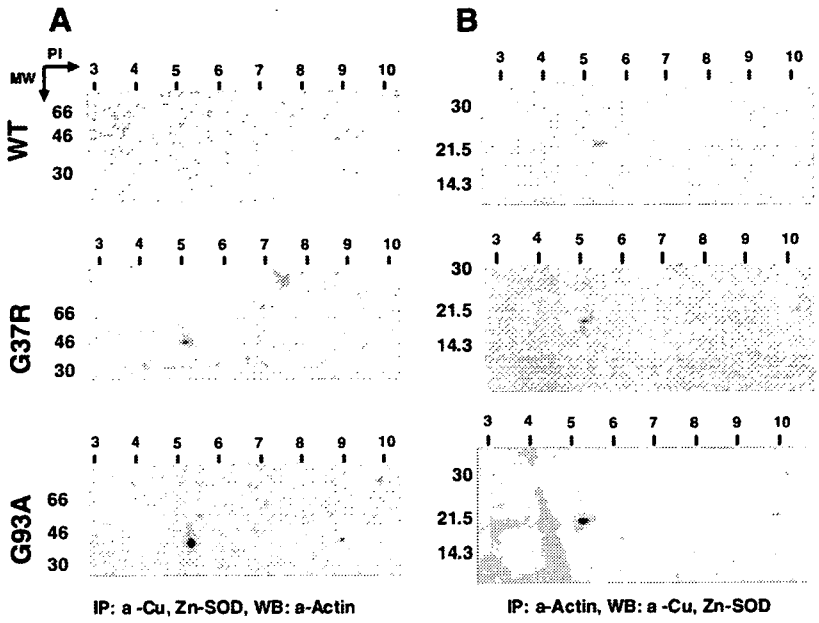

Fig. 7. Determination of Cu,Zn-SOD associated proteins. *A*: samples were immunoprecipitated with an anti-Cu,Zn-SOD antibody and subjected to 2-D gel electrophoresis (10%) and Western blot analysis using an anti-actin antibody. *B*: samples were immunoprecipitated with an anti-actin antibody and subjected to 2-D gel electrophoresis (15%) and Western blot analysis using an anti-Cu,Zn-SOD antibody.

results suggest that mutated Cu,Zn-SOD has a greater tendency to associate with actin protein.

Mutated Cu,Zn-SOD directly associate with actin in vitro. To determine whether mutated Cu,Zn-SOD directly suppressed actin polymerization, we purified wild-type and mutated Cu,Zn-SOD in a baculovirus insect cell system and performed an actin polymerization assay. In this assay, we found that both wild-type and mutated Cu,Zn-SOD did not prevent actin polymerization (data not shown). We then performed in vitro incubation of actin and Cu,Zn-SOD. Actin samples incubated with purified wild-type and mutated Cu,Zn-SOD were immunoprecipitated with anti-Cu,Zn-SOD antibody and subjected to Western blot analysis using an anti-actin antibody. As shown in Fig. 8, a band corresponding to the molecular mass of actin was observed in the mixture with the mutated Cu,Zn-SOD. These results suggest that mutated Cu,Zn-SOD directly associates with actin.

DISCUSSION

Cell cycle changes in mouse neuroblastoma N2a cells transfected with FALS-associated mutants of Cu,Zn-SOD were examined. When G37R and G93A Cu,Zn-SOD mutants were transfected into N2a cells, G_2/M arrest and significant cell growth retardation were observed. Although there were no significant changes in tubulin immunoreactivities, the mutated Cu,Zn-SOD transfectants displayed less reactivity to phalloidin than did the wild-type transfectants, indicating that actin disruption occurred in the mutant transfectants. Immunoprecipitation and 2-D gel electrophoresis followed by Western blot analysis indicated that the mutated Cu,Zn-SOD tended to associate with actin. The in vitro study in which purified Cu,Zn-SOD was incubated with actin indicated that the mutated Cu,Zn-SOD directly associated with actin. G_2/M arrest also occurred in mutated Cu,Zn-SOD-transfected NIH-3T3 cells, although the extent was much less than observed in transfectants of N2a cells (data not shown). Therefore, these phenomena are not considered to be N2a cell specific.

Mutated Cu,Zn-SOD have several enhanced activities that could be capable of selectively damaging interacting proteins or their associated organelles (5, 24, 36, 38). Investigators at our laboratory previously reported that Cu-binding affinities are decreased in mutated Cu,Zn-SOD (26) and mutated Cu,Zn-SOD are highly susceptible to nonenzymatic glycosylation, i.e., glycation (34). It is possible that actin-bound mutated Cu,Zn-SOD is glycated in vivo and reactive oxygen species could be produced via the Fenton reaction involving free Cu ions released from Cu,Zn-SOD (27). Recent reports indicate that hydrogen peroxide causes an increase in F- and G-actin oxidation and a decrease in the F-actin fraction (3, 4). The association of mutated Cu,Zn-SOD with actin might be unexpectedly toxic to the actin cytoskeleton.

Cytoskeletal changes and subsequent G_2/M arrest are commonly seen in apoptotic cells. However, when we performed the apoptotic assay by examining the DNA ladder, no significant apoptotic evidence was seen in mutated Cu,Zn-SOD-transfected N2a cells after 2-day serum starvation (data not shown).

The cytoskeletal changes observed in the mutated Cu,Zn-SOD in this study could be related to neuronal cell death observed in patients with FALS. In recent studies, researchers have reported that cytoskeletal proteins are significantly altered in ALS spinal motor neurons. For example, neurofilament

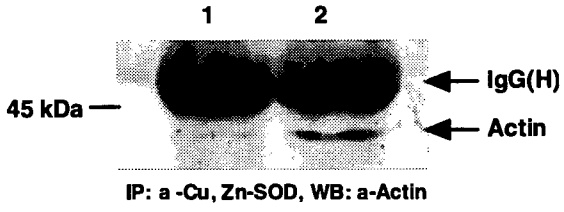

Fig. 8. In vitro association of G93A Cu,Zn-SOD with actin. After wild-type or G93A mutation, Cu,Zn-SOD (0.1 μg) was incubated with human platelet actin (0.1 μg) in actin polymerization buffer (in mM: 50 KCl, 2 $MgCl_2$, and 1 ATP) for 1 h at 24°C, and the samples were immunoprecipitated with an anti-Cu,Zn-SOD antibody and subjected to Western blot analysis using anti-actin antibody. *Lane 1*: wild-type Cu,Zn-SOD incubated with actin; *lane 2*: G93A-mutated Cu,Zn-SOD incubated with actin.

aggregation is known to be an early pathological hallmark of the disease process. Furthermore, Vukosavic et al. (35) reported that the level of β-actin decreases in the mutated Cu,Zn-SOD transgenic mice. The association of mutated Cu,Zn-SOD with actin reported in the present study could be an another important factor in cytoskeletal disruption and the apoptosis of neuronal cells in FALS.

The association of mutant Cu,Zn-SOD with actin could also be involved in the formation of aggregates that are observed in ALS. An increasing number of studies have stressed the role of mutant Cu,Zn-SOD-derived aggregation in the pathogenesis of ALS. Intracellular Cu,Zn-SOD aggregates are found in cultured motor neurons after the microinjection of mutant *Sod1* cDNA (11). Aggregates containing Cu,Zn-SOD were also detected in motor neurons and astrocytes of transgenic mice that expressed mutant *Sod1* (7). Mutant Cu,Zn-SOD aggregation into insoluble protein complexes is considered to be an early event in the pathogenic mechanism of FALS (18). Transfection studies indicated that mutant but not wild-type Cu,Zn-SOD forms cytoplasmic aggregates (18, 20). Such aggregates might interact inappropriately with other cellular components to impair cellular function. Pasinelli et al. (28) recently reported that mutant Cu,Zn-SOD-containing aggregates binds to Bcl-2 in spinal cord mitochondria, suggesting possible mechanisms of neurotoxicity of mutant Cu,Zn-SOD. Aggregates observed in ALS are also likely substrates for dynein-mediated transport and cause the disruption of microtubule-dependent axonal transport of other substrates. In addition, they are considered to stimulate neurodegeneration by overwhelming the capacity of the protein-folding chaperones and normal proteasome function. Thus the toxicity of mutant Cu,Zn-SOD could result from their propensity to aggregate. Similar mechanisms have been proposed for other degenerative diseases such as Alzheimer's disease, light-chain amyloidosis, and the spongiform encephalopathies (8). What, then, is the cause of the formation of such toxic aggregations? One possible mechanism is aberrant protein-protein interactions as demonstrated in mutant proteins in some neurodegenerative and/or neuromuscular disorders (9, 23). Kunst et al. (21) reported that G85R and G93A Cu,Zn-SOD bind to translocon-associated protein-δ (TRAP-δ) and lysyl-tRNA synthetase (KARS) using a yeast two-hybrid system. Although we were not able to identify TRAP-δ and KARS as proteins that bind to mutated Cu,Zn-SOD, it is possible that they were also present in the 2-D gels shown in Fig. 6. The mechanisms by which the mutated Cu,Zn-SOD associated with actin are currently under investigation. We assume that the structural changes or instability of Cu,Zn-SOD caused by the mutation suggested by the crystal structures (16) might be involved in this phenomenon. Further analysis of mutated Cu,Zn-SOD proteins will provide clues to their aberrant interactions with other proteins, including actin.

ACKNOWLEDGMENTS

We thank Dr. Yoshitaka Ikeda for technical support and critical discussion.

GRANTS

This work was supported by a grant from the Amyotrophic Lateral Sclerosis Association, a grant on Specific Diseases (Itoyama) from Ministry of Health and Welfare, Japan, the 21st Century COE Program of the Ministry of Education, Science, Culture, Sports, and Technology, and a Grant-in-Aid for Scientific Research (C) No. 15500237.

REFERENCES

1. **Andersen PM, Morita M, and Brown RH Jr.** *Genetics of Amyotrophic Lateral Sclerosis: An Overview*. London: World Federation of Neurology, Committee on Motor Neuron Disease, 1999.
2. **Arai K, Maguchi S, Fujii S, Ishibashi H, Oikawa K, and Taniguchi N.** Glycation and inactivation of human Cu-Zn-superoxide dismutase: identification of the in vitro glycated sites. *J Biol Chem* 262: 16969–16972, 1987.
3. **Banan A, Fitzpatrick L, Zhang Y, and Keshavarzian A.** OPC-compounds prevent oxidant-induced carbonylation and depolymerization of the F-actin cytoskeleton and intestinal barrier hyperpermeability. *Free Radic Biol Med* 30: 287–298, 2001.
4. **Banan A, Zhang Y, Losurdo J, and Keshavarzian A.** Carbonylation and disassembly of the F-actin cytoskeleton in oxidant induced barrier dysfunction and its prevention by epidermal growth factor and transforming growth factor alpha in a human colonic cell line. *Gut* 46: 830–837, 2000.
5. **Beckman JS, Carson M, Smith CD, and Koppenol WH.** ALS, SOD and peroxynitrite. *Nature* 364: 584, 1993.
6. **Bruijn LI, Becher MW, Lee MK, Anderson KL, Jenkins NA, Copeland NG, Sisodia SS, Rothstein JD, Borchelt DR, Price DL, and Cleveland DW.** ALS-linked SOD1 mutant G85R mediates damage to astrocytes and promotes rapidly progressive disease with SOD1-containing inclusions. *Neuron* 18: 327–338, 1997.
7. **Bruijn LI, Houseweart MK, Kato S, Anderson KL, Anderson SD, Ohama E, Reaume AG, Scott RW, and Cleveland DW.** Aggregation and motor neuron toxicity of an ALS-linked SOD1 mutant independent from wild-type SOD1. *Science* 281: 1851–1854, 1998.
8. **Bucciantini M, Giannoni E, Chiti F, Baroni F, Formigli L, Zurdo J, Taddei N, Ramponi G, Dobson CM, and Stefani M.** Inherent toxicity of aggregates implies a common mechanism for protein misfolding diseases. *Nature* 416: 507–511, 2002.
9. **Burke JR, Enghild JJ, Martin ME, Jou YS, Myers RM, Roses AD, Vance JM, and Strittmatter WJ.** Huntingtin and DRPLA proteins selectively interact with the enzyme GAPDH. *Nat Med* 2: 347–350, 1996.
10. **Cleveland DW and Rothstein JD.** From Charcot to Lou Gehrig: deciphering selective motor neuron death in ALS. *Nat Rev Neurosci* 2: 806–819, 2001.
11. **Durham HD, Roy J, Dong L, and Figlewicz DA.** Aggregation of mutant Cu/Zn superoxide dismutase proteins in a culture model of ALS. *J Neuropathol Exp Neurol* 56: 523–530, 1997.
12. **Farah CA, Nguyen MD, Julien JP, and Leclerc N.** Altered levels and distribution of microtubule-associated proteins before disease onset in a mouse model of amyotrophic lateral sclerosis. *J Neurochem* 84: 77–86, 2003.
13. **Ferrante RJ, Browne SE, Shinobu LA, Bowling AC, Baik MJ, MacGarvey U, Kowall NW, Brown RH Jr, and Beal MF.** Evidence of increased oxidative damage in both sporadic and familial amyotrophic lateral sclerosis. *J Neurochem* 69: 2064–2074, 1997.
14. **Fujii J, Myint T, Seo HG, Kayanoki Y, Ikeda Y, and Taniguchi N.** Characterization of wild-type and amyotrophic lateral sclerosis-related mutant Cu,Zn-superoxide dismutases overproduced in baculovirus-infected insect cells. *J Neurochem* 64: 1456–1461, 1995.
15. **Gurney ME, Pu H, Chiu AY, Dal Canto MC, Polchow CY, Alexander DD, Caliendo J, Hentati A, Kwon YW, Deng HX, Chen W, Zhai P, Sufit RL, and Siddique T.** Motor neuron degeneration in mice that express a human Cu,Zn superoxide dismutase mutation. *Science* 264: 1772–1775, 1994.
16. **Hart PJ, Liu H, Pellegrini M, Nersissian AM, Gralla EB, Valentine JS, and Eisenberg D.** Subunit asymmetry in the three-dimensional structure of a human CuZnSOD mutant found in familial amyotrophic lateral sclerosis. *Protein Sci* 7: 545–555, 1998.
17. **Hirano A, Nakano I, Kurland LT, Mulder DW, Holley PW, and Saccomanno G.** Fine structural study of neurofibrillary changes in a family with amyotrophic lateral sclerosis. *J Neuropathol Exp Neurol* 43: 471–480, 1984.
18. **Johnston JA, Dalton MJ, Gurney ME, and Kopito RR.** Formation of high molecular weight complexes of mutant Cu, Zn-superoxide dismutase in a mouse model for familial amyotrophic lateral sclerosis. *Proc Natl Acad Sci USA* 97: 12571–12576, 2000.
19. **Julien JP.** Amyotrophic lateral sclerosis: unfolding the toxicity of the misfolded. *Cell* 104: 581–591, 2001.
20. **Koide T, Igarashi S, Kikugawa K, Nakano R, Inuzuka T, Yamada M, Takahashi H, and Tsuji S.** Formation of granular cytoplasmic aggregates

in COS7 cells expressing mutant Cu/Zn superoxide dismutase associated with familial amyotrophic lateral sclerosis. *Neurosci Lett* 257: 29–32, 1998.

21. **Kunst CB, Mezey E, Brownstein MJ, and Patterson D.** Mutations in SOD1 associated with amyotrophic lateral sclerosis cause novel protein interactions. *Nat Genet* 15: 91–94, 1997.
22. **Lee PJ, Alam J, Wiegand GW, and Choi AM.** Overexpression of heme oxygenase-1 in human pulmonary epithelial cells results in cell growth arrest and increased resistance to hyperoxia. *Proc Natl Acad Sci USA* 93: 10393–10398, 1996.
23. **Li XJ, Li SH, Sharp AH, and Nucifora FC Jr, Schilling G, Lanahan A, Worley P, Snyder SH, and Ross CA.** A huntingtin-associated protein enriched in brain with implications for pathology. *Nature* 378: 398–402, 1995.
24. **Mourelatos Z, Gonatas NK, Stieber A, Gurney ME, and Dal Canto MC.** The Golgi apparatus of spinal cord motor neurons in transgenic mice expressing mutant Cu,Zn superoxide dismutase becomes fragmented in early, preclinical stages of the disease. *Proc Natl Acad Sci USA* 93: 5472–5477, 1996.
25. **Nguyen MD, Boudreau M, Kriz J, Couillard-Després S, Kaplan DR, and Julien JP.** Cell cycle regulators in the neuronal death pathway of amyotrophic lateral sclerosis caused by mutant superoxide dismutase 1. *J Neurosci* 23: 2131–2140, 2003.
26. **Okado-Matsumoto A, Myint T, Fujii J, and Taniguchi N.** Gain in functions of mutant Cu,Zn-superoxide dismutases as a causative factor in familial amyotrophic lateral sclerosis: less reactive oxidant formation but high spontaneous aggregation and precipitation. *Free Radic Res* 33: 65–73, 2000.
27. **Ookawara T, Kawamura N, Kitagawa Y, and Taniguchi N.** Site-specific and random fragmentation of Cu,Zn-superoxide dismutase by glycation reaction: Implication of reactive oxygen species. *J Biol Chem* 267: 18505–18510, 1992.
28. **Pasinelli P, Belford ME, Lennon N, Bacskai BJ, Hyman BT, Trotti D, and Brown RH Jr.** Amyotrophic lateral sclerosis-associated SOD1 mutant proteins bind and aggregate with Bcl-2 in spinal cord mitochondria. *Neuron* 43: 19–30, 2004.
29. **Rakhit R, Cunningham P, Furtos-Matei A, Dahan S, Qi XF, Crow JP, Cashman NR, Kondejewski LH, and Chakrabartty A.** Oxidation-induced misfolding and aggregation of superoxide dismutase and its implications for amyotrophic lateral sclerosis. *J Biol Chem* 277: 47551–47556, 2002.
30. **Rosen DR, Siddique T, Patterson D, Figlewicz DA, Sapp P, Hentati A, Donaldson D, Goto J, O'Regan JP, Deng HX, Rahmani Z, Krizus A, McKenna-Yasek D, Cayabyab A, Gaston SM, Berger R, Tanzi RE, Halperin JJ, Herzfeldt B, van den Bergh R, Hung WY, Bird T, Deng G, Mulder DW, Smyth C, Laing NG, Soriano E, Pericak-Vance MA, Haine J, Rouleau GA, Gusella JS, Horritz HR, and Brown RH Jr.** Mutations in Cu/Zn superoxide dismutase gene are associated with familial amyotrophic lateral sclerosis. *Nature* 362: 59–62, 1993.
31. **Rouleau GA, Clark AW, Rooke K, Pramatarova A, Krizus A, Suchowersky O, Julien JP, and Figlewicz D.** SOD1 mutation is associated with accumulation of neurofilaments in amyotrophic lateral sclerosis. *Ann Neurol* 39: 128–131, 1996.
32. **Sato Y, Takahashi M, Shibukawa Y, Jain SK, Hamaoka R, Miyagawa J, Yaginuma Y, Honke K, Ishikawa M, and Taniguchi N.** Overexpression of N-acetylglucosaminyltransferase III enhances the epidermal growth factor-induced phosphorylation of ERK in HeLaS3 cells by up-regulation of the internalization rate of the receptors. *J Biol Chem* 276: 11956–11962, 2001.
33. **Suzuki T, Oishi M, Marshak DR, Czernik AJ, Nairn AC, and Greengard P.** Cell cycle-dependent regulation of the phosphorylation and metabolism of the Alzheimer amyloid precursor protein. *EMBO J* 13: 1114–1122, 1994.
34. **Takamiya R, Takahashi M, Myint T, Park YS, Miyazawa N, Endo T, Fujiwara N, Sakiyama H, Misonou Y, Miyamoto Y, Fujii J, and Taniguchi N.** Glycation proceeds faster in mutated Cu, Zn-superoxide dismutases related to familial amyotrophic lateral sclerosis. *FASEB J* 17: 938–940, 2003.
35. **Vukosavic S, Stefanis L, Jackson-Lewis V, Guégan C, Romero N, Chen C, Dubois-Dauphin M, and Przedborski S.** Delaying caspase activation by Bcl-2: A clue to disease retardation in a transgenic mouse model of amyotrophic lateral sclerosis. *J Neurosci* 20: 9119–9125, 2000.
36. **Wiedau-Pazos M, Goto JJ, Rabizadeh S, Gralla EB, Roe JA, Lee MK, Valentine JS, and Bredesen DE.** Altered reactivity of superoxide dismutase in familial amyotrophic lateral sclerosis. *Science* 271: 515–518, 1996.
37. **Williamson TL and Cleveland DW.** Slowing of axonal transport is a very early event in the toxicity of ALS-linked SOD1 mutants to motor neurons. *Nat Neurosci* 2: 50–56, 1999.
38. **Yim MB, Kang JH, Yim HS, Kwak HS, Chock PB, and Stadtman ER.** A gain-of-function of an amyotrophic lateral sclerosis-associated Cu,Zn-superoxide dismutase mutant: An enhancement of free radical formation due to a decrease in Km for hydrogen peroxide. *Proc Natl Acad Sci USA* 93: 5709–5714, 1996.

Am J Physiol Cell Physiol 288: C1461, 2005;
doi:10.1152/ajpcell.00122.2005.

Volume 287, December 2004
Volume 56, December 2004

Page C1527–C1536. Sorkin AM, Dee KC, and Knothe Tate ML. "'Culture shock' from the bone cell's perspective: emulating physiological conditions for mechanobiological investigations." (http://ajpcell.physiology.org/cgi/content/full/287/6/C1527; doi: 10.1152/ajpcell.00059.2004). During production, the bibliography was restructured, but some changes were not accurately reflected in the corresponding in-text citations. The specific corrections are itemized here.

Page C1528: In the left column, second paragraph, last line, the reference call out 62 is incorrect; it should be (63, 91, 119). In the last line of the second column, (63) should be (68).

Page C1529: In the left column, middle of first paragraph, a reference call out 120 is incorrect; therefore, (76, 120, 126, 147) should be (76, 126, 147). In the Fig. 1 legend, (90) should be (92).

Page C1531: In the left column, first paragraph, (69, 105) should be (69, 109). In the second paragraph, (150) should be (151).

Page C1532: In the left column, first sentence, (26, 59, 149) should read as (26, 60, 149), (101) should be (102), and (86) should be (85).

Volume 288, February 2005
Volume 57, February 2005

Pages C253–C259: Takamiya R, Takahashi M, Park YS, Tawara Y, Fujiwara N, Miyamoto Y, Gu J, Suzuki K, and Taniguchi N. "Overexpression of mutated Cu,Zn-SOD in neuroblastoma cells results in cytoskeletal change" (http://ajpcell.physiology.org/cgi/content/full/288/2/C253; doi: 10.1152/ajpcell.00014.2004). In the MATERIALS AND METHODS section on page C254, in the paragraph titled "*Immunoprecipitation, two-dimensional gel electrophoresis and Western blotting*," the anti-actin antibody (from Sigma) was described as a "mouse" anti-actin antibody. In fact, this was a "rabbit" anti-actin antibody.

JOURNAL OF VIROLOGY, Aug. 2007, p. 7902–7912
0022-538X/07/$08.00+0 doi:10.1128/JVI.02675-06

Vol. 81, No. 15

Establishment of a Poliovirus Oral Infection System in Human Poliovirus Receptor-Expressing Transgenic Mice That Are Deficient in Alpha/Beta Interferon Receptor▽

Seii Ohka,[1]* Hiroko Igarashi,[1] Noriyo Nagata,[2] Mai Sakai,[1] Satoshi Koike,[3] Tomonori Nochi,[4] Hiroshi Kiyono,[4] and Akio Nomoto[1]

Department of Microbiology, Graduate School of Medicine, The University of Tokyo, 7-3-1 Hongo, Bunkyo-ku, Tokyo 113-0033,[1] Department of Pathology, National Institute of Infectious Diseases, Gakuen 4-7-1, Musashimurayama-shi, Tokyo 208-0011,[2] Department of Microbiology, Tokyo Metropolitan Institute for Neuroscience, 2-6 Musashidai, Fuchu, Tokyo 183-8526,[3] and Division of Mucosal Immunology, Department of Microbiology and Immunology, The Institute of Medical Science, The University of Tokyo, 4-6-1 Shirokanedai, Minato-ku, Tokyo 108-8639,[4] Japan

Received 4 December 2006/Accepted 8 May 2007

Poliovirus (PV) is easily transferred to humans orally; however, no rodent model for oral infections has been developed because of the alimentary tract's low sensitivity to the virus. Here we showed that PV is inactivated by the low pH of the gastric contents in mice. The addition of 3% $NaHCO_3$ to the viral inoculum increased the titer of virus reaching the small intestine through the stomach after intragastric inoculation of PV. Transgenic mice (Tg) carrying the human PV receptor (hPVR/CD155) gene and lacking the alpha/beta interferon receptor (IFNAR) gene (hPVR-Tg/*Ifnar*KO) were sensitive to the oral administration of PV with 3% $NaHCO_3$, whereas hPVR-Tg expressing IFNAR were much less sensitive. The virus was detected in the epithelia of the small intestine and proliferated in the alimentary tract of hPVR-Tg/*Ifnar*KO. By the ninth day after the administration of a virulent PV, the mice had died. These results suggest that IFNAR plays an important role in determining permissivity in the alimentary tract as well as the generation of virus-specific immune responses to PV via the oral route. Thus, hPVR-Tg/*Ifnar*KO are considered to be the first oral infection model for PV, although levels of anti-PV antibodies were not elevated dramatically in serum and intestinal secretions of surviving mice when hPVR-Tg/*Ifnar*KO were administered an attenuated PV.

Poliomyelitis is an acute disease of the central nervous system (CNS) caused by poliovirus (PV), a human enterovirus that belongs to the family *Picornaviridae*. In humans, an infection is initiated by oral ingestion of the virus, followed by multiplication in the alimentary mucosa (2, 38), from which the virus spreads through the bloodstream. Viremia is considered essential for leading to paralytic poliomyelitis in humans. By use of a PV-sensitive mouse model, previous studies (9, 44) demonstrated that after intravenous inoculation, circulating PV crosses the blood-brain barrier at a high rate, and a neural dissemination pathway from the skeletal muscle without injury is not the primary route by which the circulating virus disseminates to the CNS. Along with the blood-brain barrier pathway of dissemination, a neural pathway has been reported for humans (30), primates (11), and PV-sensitive transgenic mice (Tg) carrying the human PV receptor (hPVR/CD155) gene (31, 34); this pathway appears to be important in causing provocation poliomyelitis (9).

It has been proved that Tg carrying the hPVR gene (hPVR-Tg) are susceptible to all three PV serotypes, 1, 2, and 3 (22, 35), although mice without the hPVR gene are generally not susceptible to PV. This observation indicates that hPVR is the most important determinant of the host range of PV. After inoculation with PV by the intracerebral, intraspinal, intravenous, or intramuscular route (10, 20–22, 33–35), hPVR-Tg develop a flaccid paralysis in their limbs, which is clinically similar to human poliomyelitis. However, in contrast to its behavior in humans, PV does not replicate in the alimentary tracts of hPVR-Tg after oral administration, even in animals expressing high levels of hPVR in the intestinal epithelial cells (45). This result suggests that the expression of hPVR in the intestine is not solely responsible for the infection. It is also known that nonhuman primates are highly susceptible to PV by all routes except the oral route, yet the degree of oral susceptibility depends on the species (12). Thus, although oral infection is the most important route in humans, no adequate animal model has been established so far.

After an oral infection with PV, the virus must overcome at least three barriers before it can start to replicate efficiently in the first target cells in the small intestine: (i) the gastric acid solution, by which PV may be inactivated; (ii) inappropriate distribution of hPVR, by which PV may not be ushered to the correct target cells; and (iii) innate immunity, including interferon (IFN) signaling, by which the replication of PV may be hampered in the target cells (7). To know why orally administered PV hardly causes any paralysis in animals other than humans, we have to verify each step (see Fig. 7). In this report, barrier ii is defined as cell susceptibility and barrier iii is defined as cell permissivity.

To control poliomyelitis, attenuated PV strains of all three serotypes have been developed and used effectively as oral polio vaccines (37, 39). The attenuated Sabin strains can rep-

* Corresponding author. Mailing address: Department of Microbiology, Graduate School of Medicine, The University of Tokyo, 7-3-1 Hongo, Bunkyo-ku, Tokyo, 113-0033, Japan. Phone: 81-3-5841-3410. Fax: 81-3-5841-3374. E-mail: seii@m.u-tokyo.ac.jp.

▽ Published ahead of print on 16 May 2007.

licate well only in the alimentary tracts of humans without showing neuropathogenicity, enough to elicit neutralizing antibodies against PV after oral administration.

Picornaviruses are sensitive to IFNs (3, 5, 24, 28, 46). IFNs play an essential role in the innate immune antiviral response. Recently, Ida-Hosonuma et al. (13) found that deletion of the IFN-α/β receptor (IFNAR) gene in hPVR-Tg (hPVR-Tg/*Ifnar*KO) resulted in the disruption of IFN-α/β signaling (27), which is an important determinant of the tissue tropism and pathogenicity of PV. Similarly, it has been reported that IFN-α/β plays an important role in the pathogenicity and tissue tropism of some viruses, including coxsackievirus and Theiler's virus in the *Picornaviridae* (6, 8, 26, 36, 42). These results suggest that not only hPVR (cell susceptibility) but also IFN-α/β (cell permissivity) contributes to the pathogenicity and tissue tropism of PV.

In this paper, we have clarified the instability of the virus in the gastric environment, where the low pH of the gastric contents inactivates PV. Furthermore, using hPVR-Tg with or without IFNAR expression, we have shown that IFN-α/β plays a key role in preventing PV from replicating in the intestines of mice.

MATERIALS AND METHODS

Viruses and cells. The virulent Mahoney strain [PV1(M)OM] and the avirulent Sabin 1 strain [PV1(Sab)IC-0] of type 1 PV derived from infectious cDNA clones pOM1 (41) and pVS(1)IC-0(T) (19), respectively, were employed in this study. As other virulent strains, Lansing (type 2) and Leon (type 3) were used.

African green monkey kidney (AGMK) cells were grown in Dulbecco's modified Eagle's medium (DMEM) supplemented with 5% newborn calf serum and were used for the preparation of viruses, transfection with infectious cDNA clones, and plaque assays.

Tg. The Tg strains used in this paper have been described previously (13). In brief, mice of a transgenic strain, ICR-PVRTg21 (21, 22), were backcrossed with C57BL/6 mice, and homozygotes with the C57BL/6 background (C57BL/6-PVRTg21) were produced. In this report, strain C57BL/6-PVRTg21 is referred to as PVRTg21. A129 mice, deficient in the *Ifnar* gene (27), were backcrossed with C57BL/6 mice and then further crossed with PVRTg21 or MPVRTg25-61 (MPVRTg25) (43). MPVRTg25 express hPVR under the control of the mouse PVR homolog (MPH) (25) regulatory gene. $PVR^{+}/^{+}$ $Ifnar^{-}/^{-}$ mice were obtained by intercrossing these PVRTg21/*Ifnar*KO (13) or MPVRTg25/*Ifnar*KO. All mice used were free of specific pathogens and were 7 to 10 weeks old. Mice were treated according to the guidelines for the Care and Use of Laboratory Animals of The University of Tokyo.

Assay of PV inactivation. PV1(M)OM (5 μl) was incubated at 37°C or 0°C for the periods indicated with 45 μl of each solution, and then the titer of virus was determined by a plaque assay. The pH 1 solution was 0.1 N HCl, the pH 2 solution was 0.01 N HCl, the pH 3 solution was 0.001 N HCl, and the pH 7 solution was saline. The pH of each solution was measured using pH test paper at the start and end points of the incubation.

Administration of viruses. For sampling of the gastric contents, mice were fasted overnight and then anesthetized with an intraperitoneal injection of 300 to 400 μl of ketamine (10 mg/ml) and xylazine (0.2 mg/ml) in saline. The stomach was exposed, and the pylorus was ligated with silk thread. The mice were inoculated with 200 μl of saline by using a gastric tube, and the gastric contents were collected. The gastric contents were centrifuged at 15,000 rpm for 10 min, and the supernatant was filtered. The filtrate was used for the experiments.

The viruses were administered orally using quantitative water bottles (Drinko-Measurer DM-G1; O'Hara & Co., Ltd., Japan). First, mice were fasted overnight, and then 2 ml of a viral solution containing 3% $NaHCO_3$ per mouse was administered within 24 h using the water bottles. The time point for starting the administration was taken as time zero. Twenty-four hours after the administration was started, the quantitative water bottles were replaced with conventional water bottles.

Recovery of viruses from tissues. For determination of the titer of virus in the tissues, the mice inoculated with the viruses were anesthetized and whole blood was recovered from the right ventricle. Immediately, the mice were perfused with saline through the left ventricle, and the tissues were excised. The tissues were homogenized in DMEM without serum to prepare a 10% emulsion. The homogenates were centrifuged to remove any debris, and the supernatant containing the virus was subjected to a plaque assay.

Labeling of PV. PV was purified by a protocol described previously (16). HeLa S3 cells were infected with PV1(M)OM at a multiplicity of infection of 10. The cells were harvested at 7 h postinfection, and the virus was purified from cytoplasmic extracts of the infected cells by using DEAE-Sepharose CL-6B (GE Healthcare Bio-Sciences KK) followed by centrifugation on a sucrose density gradient and CsCl equilibrium centrifugation. Purified virus was desalted by gel filtration on a PD-10 column (GE Healthcare Bio-Sciences KK) equilibrated with phosphate-buffered saline [PBS(−)] (per liter, 8.00 g NaCl, 1.15 g Na_2HPO_4, 0.20 g KCl, 0.10 g $MgCl_2 \cdot 6H_2O$, 0.20 g KH_2PO_4 [pH 7.4]). The concentration of poliovirions was determined by measuring the absorbance at 260 nm, where 1.0 optical density unit is regarded as equivalent to 9.4×10^{12} virions. The labeling of the virus is based on a protocol kindly provided by Lucas Pelkmans (32). PV (0.4 mg at 0.4 mg/ml) was labeled with 0.39 μl of Alexa Fluor 555-succinimidyl ester (10 mg/ml in dimethyl sulfoxide) according to the manufacturer's instructions (Invitrogen). These fluorophores react exclusively with free amines, resulting in a stable carboxamide bond. Labeled virus was repurified with NAP5 columns (GE Healthcare Bio-Sciences KK), dialyzed against PBS(−), and stored at −80°C. The labeling ratio was 14 mol of dye per mol of virus, and the specific infectivity of labeled virus was not reduced.

Detection of fluorescently labeled virus. After the MPVRTg25/*Ifnar*KO were anesthetized as described above, the intestines were exposed. The small intestine was ligated with silk thread at two points. Labeled virus was injected into the small intestine between the knots of the thread. One hour later, the injected portion of the small intestine was excised and washed with saline. The small intestine was directly observed under a confocal laser scanning microscope (LSM510; Carl Zeiss MicroImaging GmbH). For preparation of fixed tissue sections, the small intestine was immediately frozen in OCT compound (Sakura Fine Technical Co., Ltd.). Tissue sections were prepared by using a Jung CM3000 cryostat (Leica Instruments GmbH), mounted on 3-aminopropyltriethoxysilane-coated slides (Matsunami Glass Industries, Ltd.), and dried. All the staining procedures were performed at room temperature. First, the specimens were fixed in PBS(−) containing 2% paraformaldehyde for 1 min and washed four times in PBS(−). After treatment with 1.5% normal goat serum in PBS(−) for 20 min, 1 μg/ml of fluorescein isothiocyanate-labeled *Ulex europaeus* agglutinin-1 (UEA-1) was applied, and the specimens were incubated for 15 min and then washed with PBS(−). Nucleic acids were stained with 50 nM SYTO59 (Invitrogen). The sections were mounted with 80% (vol/vol) glycerol in PBS(−) and analyzed with a confocal laser scanning microscope.

Neutralizing assay. PVRTg21 and PVRTg21/*Ifnar*KO were orally administered 3×10^8 PFU of Sabin 1 along with 3% $NaHCO_3$ within 37 h by using quantitative water bottles. As a positive control, PVRTg21/*Ifnar*KO were intravenously injected with 1×10^5 PFU of Sabin 1. Twenty-one days after the administration, whole blood was collected from each mouse and serum was prepared after centrifugation. After incubation of the serum at 45°C for 1 h, 100 PFU of Sabin 1 in 100 μl was mixed with 100 μl of serially diluted serum and incubated for 1 h at 37°C. The virus-serum mixture was subjected to a plaque assay. Neutralizing activity is expressed as the maximum denominator for the dilution that can neutralize 100 PFU of Sabin 1.

RESULTS

Mouse gastric contents can inactivate PV. hPVR-Tg are much less susceptible to orally administered PV than humans. To explain this, we examined the stability of the virus during its passage through the mouse stomach after oral administration of PV. First, we examined whether a mouse gastric solution can inactivate PV. Under anesthesia, the pylorus was ligated and 200 μl of saline was inoculated using a gastric tube. Right after the inoculation, the gastric contents were collected, and the supernatant obtained by centrifugation was used as a gastric solution. As shown in Fig. 1A, 2×10^5 PFU of PV1(M)OM was incubated at 37°C or 0°C for the times indicated with or without the gastric solution from Tg or non-Tg. When PV was incubated at 37°C with the gastric solution from Tg or non-Tg, the titer of the virus was apparently reduced, whereas PV incubated with saline at 37°C for 4 h or PV just after mixing with the gastric solution showed no reduction. These results

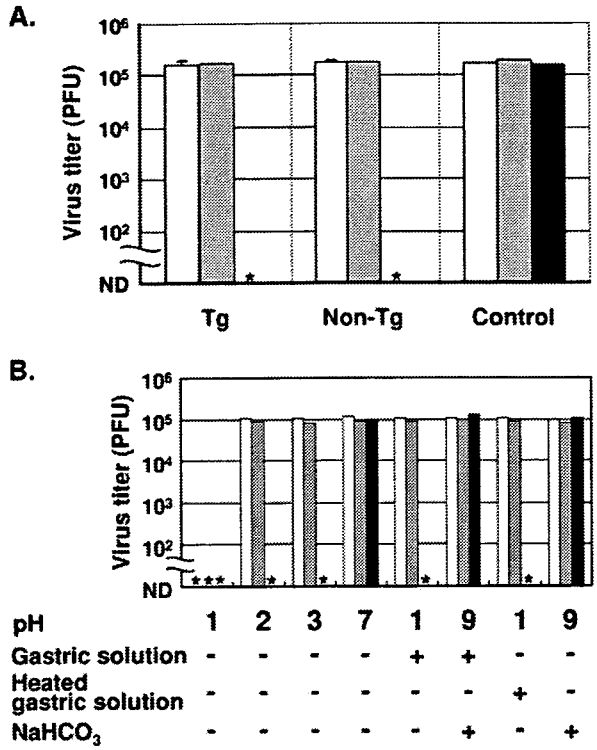

FIG. 1. Inactivation of PV with a mouse gastric solution. (A) PV1(M)OM at 2×10^5 PFU/5 μl was incubated at 37°C or 0°C for the periods indicated with or without 45 μl of a gastric solution from PVRTg21 (Tg) or C57BL/6 (non-Tg) mice, and then the titer of virus was determined by a plaque assay. As a control, PV was incubated with 45 μl of saline. Three animals were used per group. (B) PV1(M)OM at 1×10^5 PFU/5 μl was incubated at 37°C or 0°C for the periods indicated with 45 μl of each solution. After the incubation, the titer of virus was determined by a plaque assay. Open bars, samples just after mixing; solid bars, incubation at 37°C for 4 h; shaded bars, incubation at 0°C for 4 h. Asterisks, nondetectable titers. ND, not detected.

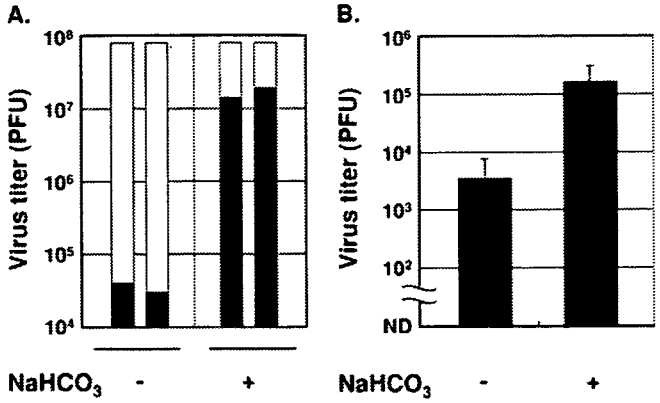

FIG. 2. Effect of passage through gastric contents on the virus titer after intragastric inoculation of mice with PV. (A) The effect of mouse gastric contents in the stomach on the retention of PV was examined. Under anesthesia, the pylorus was ligated and MPVRTg25 were intragastrically inoculated with 7.8×10^7 PFU of PV1(M)OM/500 μl with or without 3% $NaHCO_3$ by using a gastric tube. Five minutes after inoculation, the gastric contents were quickly recovered and the virus was detected by a plaque assay. Each bar represents an individual mouse. The black area indicates the titer detected in the gastric contents, and the white area indicates the decrease in the inoculated titer. (B) The rate of recovery of the virus from the small intestines of MPVRTg25 was examined after intragastric inoculation with 7.8×10^7 PFU of PV1(M)OM/500 μl with or without 3% $NaHCO_3$. Four hours after the inoculation, the contents of the small intestinal lumen were recovered and the virus was detected by a plaque assay. ND, not detected.

suggest that the gastric solution inactivated PV at 37°C independently of hPVR expression in mice.

Next, we investigated which factor influenced the inactivation. To examine the effect of low pH, 1×10^5 PFU of PV1(M)OM was incubated either with an HCl-containing solution at pH 1, pH 2, or pH 3, with saline (pH 7), or with the gastric solution, with or without $NaHCO_3$, either unheated or heated to inactivate the enzymatic activities. The gastric solution had a pH of ~1 without supplementation and a pH of 9 after it was mixed with $NaHCO_3$. As shown in Fig. 1B, PV was inactivated by the pH 2 and pH 3 solutions, as well as by the gastric solution after incubation at 37°C, but not by saline (pH 7). With the pH 1 solution, PV was inactivated without incubation at 37°C or 0°C. These results suggest that a low pH can inactivate PV. To confirm the effect of the low pH, the gastric solution with $NaHCO_3$ was incubated with PV. The pH 9 gastric solution did not inactivate PV even after incubation at 37°C. As a control, a saline solution with $NaHCO_3$ (pH 9) was examined; it had no effect on the viral titer. These results suggest that the low pH of the gastric solution leads to inactivation of the virus. When HEPES was used instead of $NaHCO_3$ to bring the viral solution to a pH of 9, the titer of virus was not decreased, either (data not shown). This result further supports the dependence of the PV-inactivating effect on a low pH. Finally, our experiment aimed to determine whether gastric enzymatic activities affect the infectivity of the virus. The enzymatic activities in the gastric solution were eliminated by heating at 95°C for 5 min. The heated gastric solution inactivated the virus after incubation at 37°C similarly to the unheated gastric solution without $NaHCO_3$. This result suggests that the enzymatic activities in the gastric solution do not affect the infectivity of PV under the conditions used.

Efficient delivery of PV to the intestine after intragastric inoculation with a pH neutralizer. To examine the survival rate of the virus at a low pH in the gastric environment in vivo, an assay of infectious PV was conducted after the virus was incubated in the stomach (Fig. 2A). Under anesthesia, the pylori were ligated and the mice were intragastrically inoculated with 7.8×10^7 PFU of PV/500 μl with or without 3% $NaHCO_3$ by using a gastric tube. Five minutes after inoculation, the gastric contents were quickly recovered and the titer of the virus was determined by a plaque assay. When the mice were inoculated with PV without 3% $NaHCO_3$, the titer was less than 0.1% of the original amount inoculated. On the other hand, when the mice were inoculated with PV together with 3% $NaHCO_3$, around 20% of the inoculated virus was recovered from the stomach. These results suggest that PV can be inactivated by gastric contents in vivo similarly to the inactivation in vitro (Fig. 1). As shown in Fig. 1B, the virus with the gastric solution containing 3% $NaHCO_3$ exhibited no loss of titer, whereas the virus inoculated intragastrically with 3% $NaHCO_3$ showed an 80% loss of titer in vivo (Fig. 2A). The gastric solution used for the in vitro experiments had been diluted with saline, which may have resulted in the minor effect on the inactivation of PV.

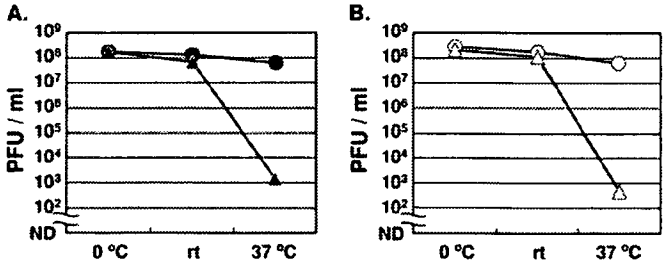

FIG. 3. PV titer after incubation for 24 h with or without $NaHCO_3$. A total of 1.5×10^8 PFU/ml of PV1(M)OM (A) or Sabin 1 (B) was incubated at the indicated temperatures for 24 h with (triangles) or without (circles) 3% $NaHCO_3$. The titer of virus after incubation was determined by a plaque assay. rt, room temperature. ND, not detected.

Next, we examined how much virus can reach the small intestine from the stomach after intragastric inoculation using a gastric tube. The rate of recovery of the virus from the small intestine was examined after intragastric inoculation of 7.8×10^7 PFU of PV with or without 3% $NaHCO_3$ by using a gastric tube. Four hours after inoculation, the contents of the entire small intestine were recovered and the titer of the virus was determined by a plaque assay (Fig. 2B). For mice inoculated with PV without 3% $NaHCO_3$, approximately 10^3 PFU/small intestinal lumen was recovered, whereas for mice inoculated with PV together with 3% $NaHCO_3$, about 10^5 PFU/small intestinal lumen was recovered. These results indicate that $NaHCO_3$ increased the recovery of the virus from the small intestinal lumen after intragastric inoculation with PV.

To know whether there is a reduction in the titer of the virus during the oral administration period (24 h), the stability of PV with 3% $NaHCO_3$ after 24 h was examined. The pH of a 3% $NaHCO_3$ solution was measured by pH test paper and determined to be 9. The titer was examined after incubation for 24 h at 0°C, room temperature, or 37°C (Fig. 3A and B). When PV1(M)OM was incubated with 3% $NaHCO_3$ or with H_2O, the titer did not decrease at 0°C or at room temperature. On the other hand, incubation of PV1(M)OM with 3% $NaHCO_3$ at 37°C reduced the titer by approximately 5 orders of magnitude, whereas incubation with H_2O at this temperature caused only about a 1-log-unit reduction (Fig. 3A). As for Sabin 1, when the virus was incubated at 0°C with 3% $NaHCO_3$ or with H_2O, no reduction in the titer was observed, whereas incubation at a higher temperature resulted in a reduction in the titer. Incubation of Sabin 1 with 3% $NaHCO_3$ or with H_2O at room temperature caused about a twofold reduction in the titer compared to that at 0°C. At 37°C, incubation of Sabin 1 with 3% $NaHCO_3$ reduced the titer by roughly 6 orders of magnitude, whereas incubation with H_2O caused only about a threefold reduction (Fig. 3B). These results suggest that incubation at room temperature for 24 h has only a minor effect on the titer and that incubation at 37°C for 24 h decreases the titer more severely, especially when the viral solution contains $NaHCO_3$. The relatively high pH of the 3% $NaHCO_3$ solution might have led to the instability of the viral RNA genome and virion particle. As for PV type 2 and 3 strains, incubation with 3% $NaHCO_3$ had only a minor effect on Leon, but Lansing showed a ~1-log-unit decrease in the titer after incubation with $NaHCO_3$ even at room temperature for 24 h (data not shown). These results suggest that the stability of PV with $NaHCO_3$ depends on the viral strain.

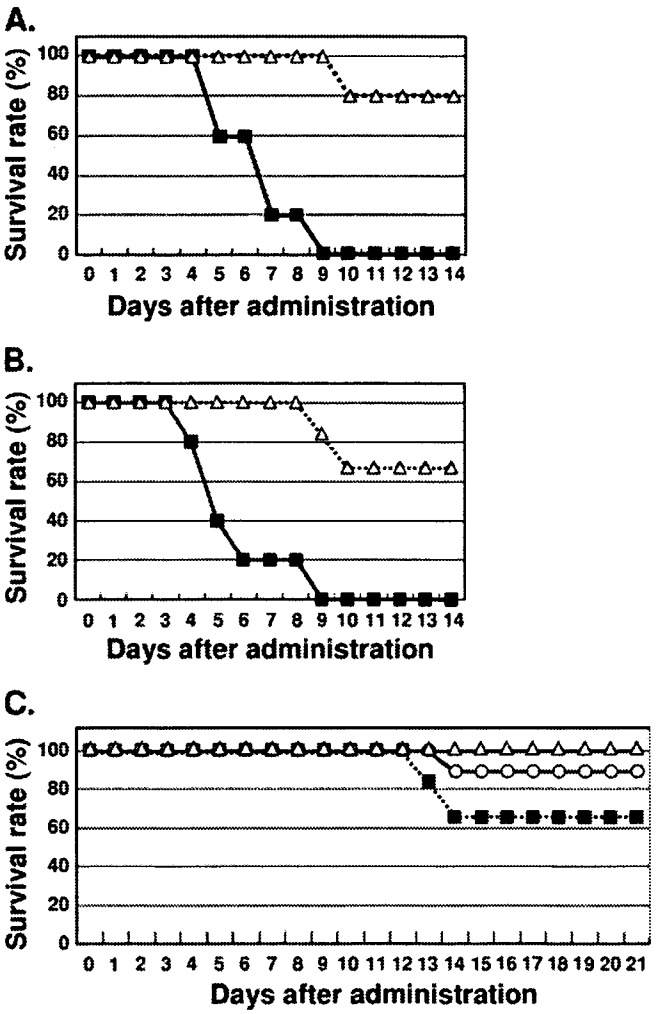

FIG. 4. Survival rates of mice after oral administration of PV. (A and C) PVRTg21/*Ifnar*KO (solid squares) or PVRTg21 (open triangles) were orally administered 3×10^8 PFU/2 ml of PV1(M)OM (A) or Sabin 1 (C), and the rate of survival was determined. Alternatively, PVRTg21/*Ifnar*KO were intravenously injected (open circles) with 1×10^5 PFU of Sabin 1/100 μl (C). Five (A), six (C) (oral administration), or nine (C) (intravenous injection) mice were observed for each group. (B) Similarly, MPVRTg25/*Ifnar*KO (solid squares) or MPVRTg25 (open triangles) were orally administered 3×10^8 PFU of PV1(M)OM/2 ml. Five or six mice were observed per group. The rate of survival was determined.

Effects of IFN-α/β signaling on the cell permissivity of orally ingested PV. To test whether PV orally ingested with 3% $NaHCO_3$ can cause paralysis in hPVR-Tg, PV with 3% $NaHCO_3$ was orally administered to PVRTg21 or to PVRTg21/*Ifnar*KO, which are deficient in *Ifnar*. To eliminate the possibility that the gastric tube might damage epithelia in the esophagus, 3×10^8 PFU of PV1(M)OM with 3% $NaHCO_3$ was orally administered without using a gastric tube. Eighty percent of PVRTg21 survived, whereas all the PVRTg21/*Ifnar*KO showed paralysis and died within 9 days of PV administration (Fig. 4A). These results suggest that PVRTg21/*Ifnar*KO are more susceptible to orally administered PV1(M)OM than PVRTg21. The susceptibility of

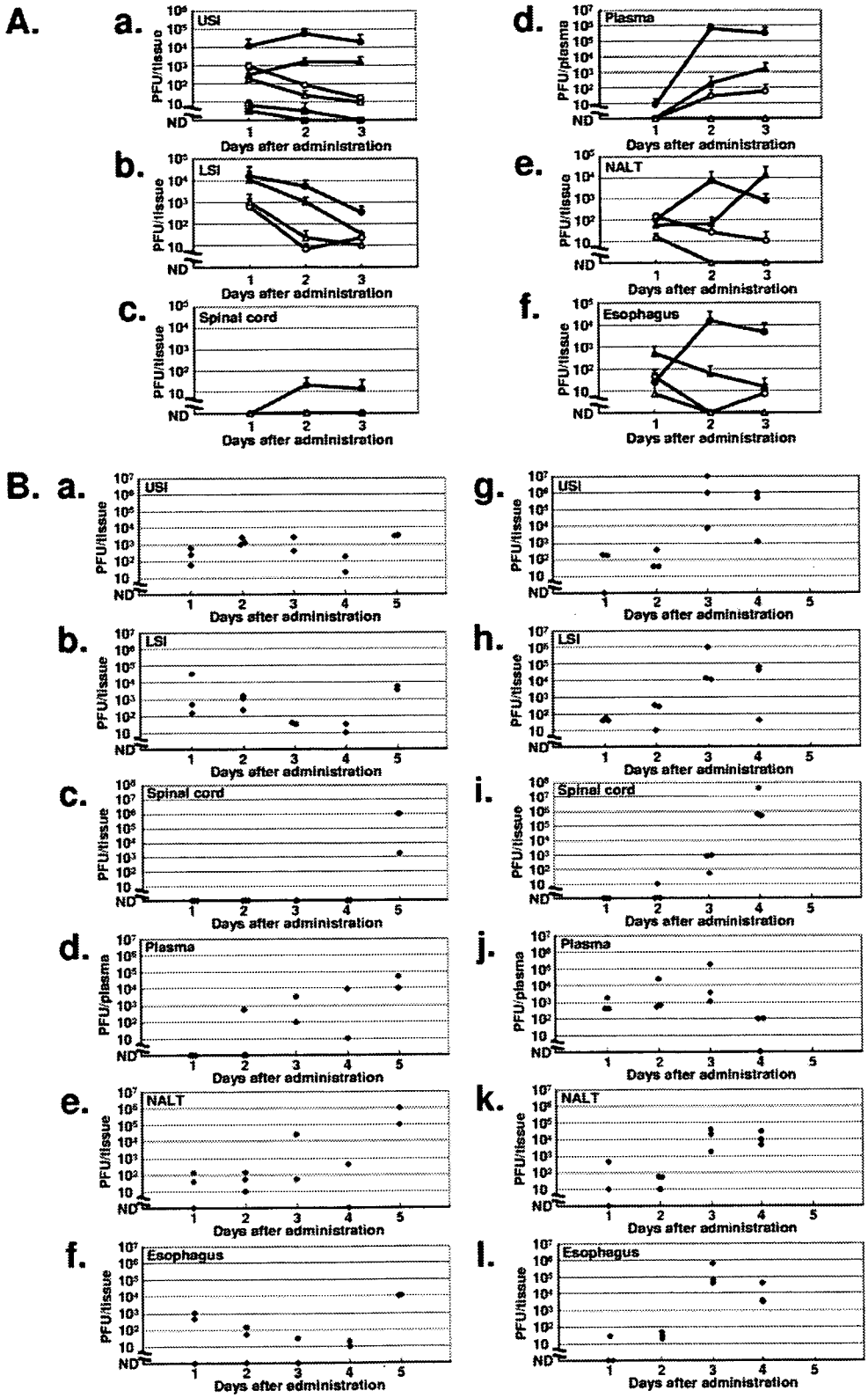

FIG. 5. Titers of PV recovered in tissues after oral administration of PV. (A) Virus was extracted from tissues of mice (PVRTg21 [open triangles], PVRTg21/*Ifnar*KO [solid triangles], MPVRTg25 [open circles], MPVRTg25/*Ifnar*KO [solid circles], C57BL/6 [open squares], and C57BL/6/*Ifnar*KO [solid squares]) 1, 2, and 3 days after the administration of 3×10^8 PFU of PV1(M)OM/2 ml. The vertical axis shows the amount (PFU) of PV detected in tissues by the plaque assay. USI, upper small intestine; LSI, lower small intestine. (B) Virus was extracted from each tissue of PVRTg21/*Ifnar*KO every 24 h after oral administration of 3×10^8 PFU of PV1(M)OM/2 ml (a to f) or intravenous injection of 1×10^5 PFU of PV1(M)OM/100 μl (g to l). Each point indicates one mouse. ND, not detected.

PVRTg21/*Ifnar*KO is dependent on the titer of virus (data not shown).

To confirm the effect of IFN signaling on the pathogenicity of orally administered PV in mice, another Tg strain (MPVRTg25) was examined, because hPVR is apparently detected in the small intestine and liver of MPVRTg25 by Western blotting (43). MPVRTg25 and MPVRTg25/*Ifnar*KO were orally administered PV with 3% $NaHCO_3$ without using a gastric tube, and the clinical symptoms were observed (Fig. 4B). In agreement with the results obtained with PVRTg21 and PVRTg21/*Ifnar*KO, all the MPVRTg25/*Ifnar*KO died whereas only 33% of MPVRTg25 died. These results suggest that MPVRTg25/*Ifnar*KO are more susceptible to oral administration of PV than MPVRTg25. These findings further support the notion that IFN signaling contributes to cell permissivity in mice orally administered PV. As for the clinical symptoms, MPVRTg25/*Ifnar*KO tend to show hepatocirrhosis rather than paralysis, and it is highly possible that these mice died of a hepatic disorder. Nevertheless, one can observe paralysis after intracerebral inoculation of MPVRTg25/*Ifnar*KO (data not shown). This result suggests that the virus can replicate in the CNS and cause paralysis even in MPVRTg25/*Ifnar*KO.

When PVRTg21/*Ifnar*KO or PVRTg21 were orally administered Sabin 1 with 3% $NaHCO_3$ without use of a gastric tube, more than 30% of PVRTg21/*Ifnar*KO showed paralysis and died, whereas all the PVRTg21 survived for 21 days (Fig. 4C). These results suggest that PVRTg21/*Ifnar*KO were more susceptible to oral administration of Sabin 1 than PVRTg21. PVRTg21/*Ifnar*KO also showed susceptibility to the type 2 strain Lansing or the type 3 strain Leon despite the fact that that Lansing was less pathogenic than PV1(M)OM or Leon (data not shown). Together with these results, our study strongly suggested that IFN signaling plays a key role in cell permissivity following oral administration of PV, although we cannot exclude the possibility that components of the innate immune system other than IFN-α/β affect the cell permissivity.

Time course of the replication of PV in tissues after oral administration. To assess the ability of PV to replicate in different tissues after oral administration, the titers of the virus in the small intestine, colon, nasopharynx-associated lymphoid tissue (NALT), esophagus, spinal cord, and plasma were determined at 1, 2, and 3 days after administration to mice. PV was orally administered to PVRTg21, PVRTg21/*Ifnar*KO, MPVRTg25, MPVRTg25/*Ifnar*KO, C57BL/6, and C57BL/6/*Ifnar*KO, and the tissues were excised each day after administration. The tissues were then homogenized, and the titers of the virus in the solutions were determined by a plaque assay (Fig. 5A). In all the tissues tested, titers were always higher in *Ifnar* knockout hPVR-Tg than in *Ifnar*-expressing hPVR-Tg. For instance, the titers were higher in PVRTg21/*Ifnar*KO than in PVRTg21, and similarly, they were higher in MPVRTg25/*Ifnar*KO than in MPVRTg25 (Fig. 5Aa to c, e, and f). As for C57BL/6/*Ifnar*KO and C57BL/6 mice, the titers in the upper small intestine were negligible (Fig. 5Aa). These results suggest that PV can replicate in all of the tissues examined more efficiently in *Ifnar* knockout mice than in *Ifnar*-expressing mice.

As for plasma, the virus caused viremia from the second day in PVRTg21/*Ifnar*KO, MPVRTg25, and MPVRTg25/*Ifnar*KO (except for one animal that showed slight viremia on the first day) (Fig. 5Ad). The results imply that the virus leaks into the blood after replicating in tissues, probably the alimentary tract, because little virus was detected in plasma on the first day.

We next investigated the chronological titer of the virus in different tissues after an oral or systemic challenge (Fig. 5B). When PVRTg21/*Ifnar*KO were intravenously inoculated with PV1(M)OM, the virus had started replicating extensively in all tissues examined on the third day (Fig. 5Bg to l). Almost all the mice injected intravenously with the virus developed paralysis and died on the fifth day (data not shown). Following oral administration of PV1(M)OM to PVRTg21/*Ifnar*KO, all the tissues examined showed a burst of proliferation of the virus on the fifth day (Fig. 5Ba to f), and the mice began to die on the fifth day (Fig. 4A). These findings indicate that the burst of replication after oral administration may be due to the virus that appeared on the second day in the bloodstream, because such a burst took 3 days after the intravenous injection. It seems feasible that the paralysis after oral administration of the virus is mainly due to the circulating virus that invaded from the alimentary tract.

Inoculated PV was incorporated into mouse small intestinal epithelia. To examine which kind of cells in the alimentary tract incorporate the virus, fluorescently labeled PV was injected into the ligated small intestine in MPVRTg25/*Ifnar*KO. One hour after the injection, the ligated tissue was subjected to confocal laser scanning microscopic analysis. As shown in Fig. 6Ab and c, the virus was detected inside the microvillus, whereas no fluorescence was detected in the small intestine without the injection (Fig. 6Ae and f). When the intestine was observed after frozen sectioning, the virus was detected in the cytoplasm of the epithelial cells in the microvilli (Fig. 6Bd and e). No fluorescence was detected in the small intestine without injection of the virus (Fig. 6Bi and j). These results suggest that the virus inside the cavity of the small intestine can be incorporated into the epithelial cells. It is highly possible that the incorporated virus starts to replicate in these epithelial cells. To further clarify which kinds of cells incorporate the virus from the intestinal cavity, fluorescently labeled UEA-1 (specific for α-L-fucose residues) was used, since UEA-1 has been shown to possess high affinity for selected intestinal epithelial cells, including mouse microfold (M) cells and goblet cells (4, 17). As shown in Fig. 6C, PV was not detected in the UEA-1-positive fraction of epithelial cells. On the other hand, the cells that contained PV were the UEA-1-negative fraction in the epithelia (Fig. 6B). It has been reported that some microorganisms, such as *Salmonella enterica* serovar Typhimurium and *Yersinia pseudotuberculosis*, can be efficiently incorporated into M cells under similar experimental conditions (15). These results suggest that in the IFN-α/β-free environment of the intestinal epithelium, PV is incorporated into the UEA-1-negative fraction of epithelial cells, although we cannot exclude the possibility that M cells are involved in the dissemination of the virus and the subsequent infection process.

Oral administration of attenuated PV did not effectively generate neutralizing antibodies in hPVR-Tg/*Ifnar*KO. Inasmuch as orally administered PV is incorporated into the intestinal epithelium and starts replicating in hPVR-Tg/*Ifnar*KO, it is important to examine whether oral administration of attenuated PV can induce the production of neutralizing antibodies in mice. To this end, attenuated PV was orally administered to

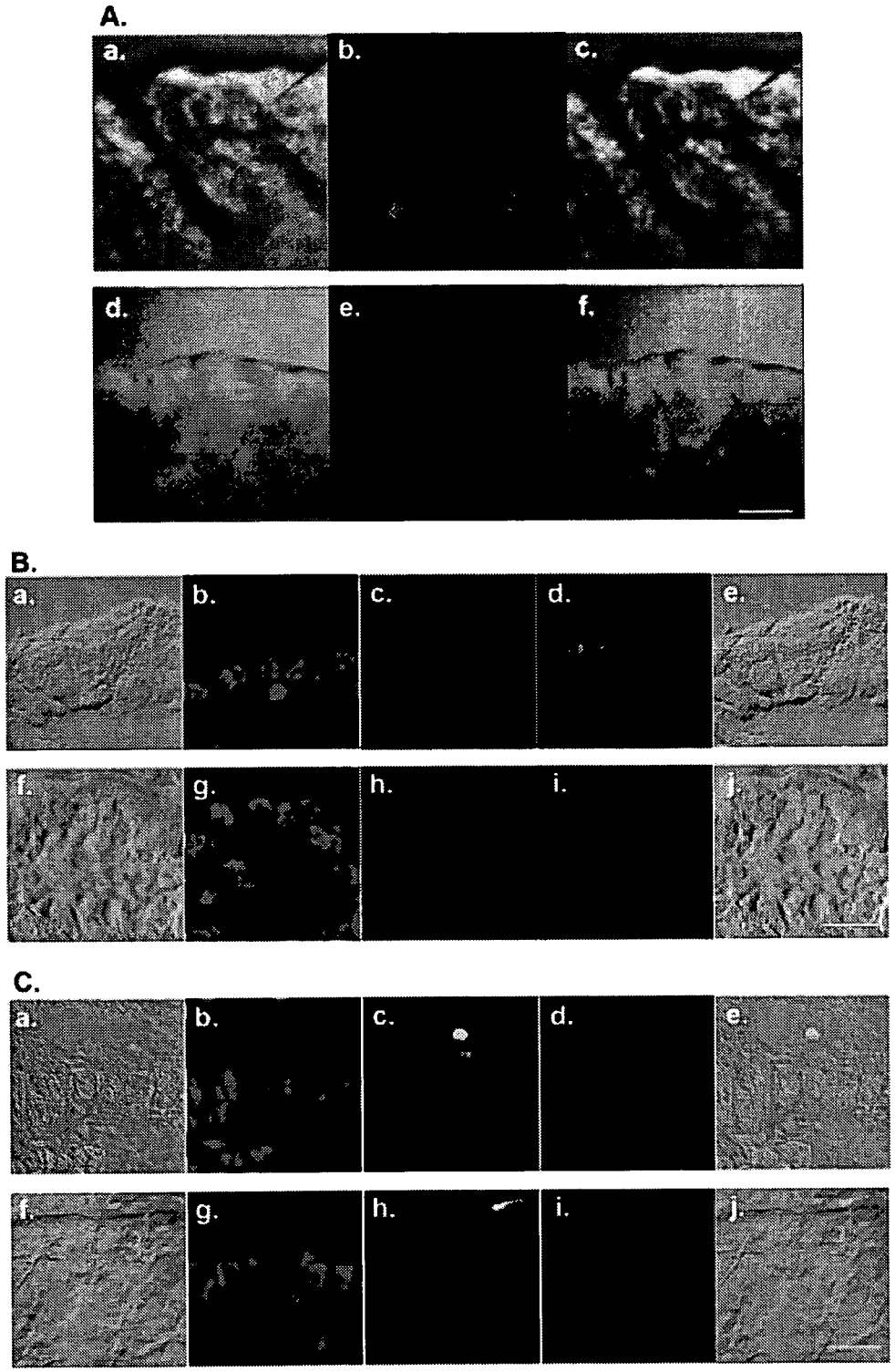

FIG. 6. Fluorescently labeled PV is detected in intestinal epithelia. Alexa Fluor 555-labeled PV1(M)OM (1.5×10^7 PFU/10 μl) was injected into the ligated small intestines of MPVRTg25/*Ifnar*KO (top row of images in each panel). PV-negative controls were also used (bottom row in each panel). One hour after injection, the ligated portion was excised and subjected to confocal laser scanning microscopy. Intestines were observed without (A) or with (B and C) fixation and frozen sectioning. (B) UEA-1-negative epithelia; (C) epithelia that contain UEA-1-positive cells. Red, Alexa Fluor 555-labeled PV1(M)OM (Ab, c, e, and f; Bd, e, i, and j; Cd, e, i, and j); blue, nuclei (Bb, e, g, and j; Cb, e, g, and j); green, fluorescein isothiocyanate-labeled UEA-1 (Bc, e, h, and j; Cc, e, h, and j). Aa and d, Ba and f, and Ca and f show bright-field images only. Ac and f, Be and j, and Ce and j show merged images of bright-field and fluorescence micrographs. Bars, 100 μm.

TABLE 1. PV-neutralizing activity in serum after oral administration of Sabin 1

Mouse strain	Substance	Route of administration	Amt of immunizing virus (PFU/mouse)	Neutralizing activity[a]
PVRTg21/*Ifnar*KO	DMEM	Oral	0	0/6
	Sabin 1	Oral	3×10^8	0/4
	Sabin 1	Intravenous	1×10^5	8/8
PVRTg21	Sabin 1	Oral	3×10^8	0/6

[a] Expressed as the number of mice whose serum showed neutralizing activity (≥16)/number of mice examined.

PVRTg21/*Ifnar*KO or PVRTg21. Serum was collected 21 days after virus administration, and the neutralizing activity in the serum was assayed. In the case of PVRTg21/*Ifnar*KO, all the mice showed neutralizing activity after intravenous inoculation of 10^5 PFU of Sabin 1 whereas no mouse showed neutralizing activity after oral administration of 3×10^8 PFU of the strain or DMEM (Table 1), although the virus was detected in the intestine until 4 days after oral administration of Sabin 1 (data not shown). As for PVRTg21, no mouse showed neutralizing activity after oral administration of 3×10^8 PFU of Sabin 1. Similar results were obtained for MPVRTg25/*Ifnar*KO after oral administration of the strain (data not shown). These results suggest that oral administration of Sabin 1 to PVRTg21/*Ifnar*KO or MPVRTg25/*Ifnar*KO was ineffective at raising the neutralizing activity.

DISCUSSION

Some of the recent outbreaks in areas certified as being clear of polio were caused by a circulating vaccine-derived PV that had mutated from the oral polio vaccine used to prevent polio (18). This suggests to us a need to develop new polio vaccines or antipolio drugs for the control of polio outbreaks. For that purpose, it is necessary to establish a useful animal model that mimics the natural infection route and subsequent disease development in humans in order to evaluate candidate vaccines or drugs.

A paper about the effects of pH on PV infectivity (40) indicates that PV can be easily inactivated at pH 3.0 or 9.0 at 30°C, but it depends on the buffers. This means that, at least at pH 3.0 or 9.0, the stability of viral infectivity is determined by the stability of the virions in particular buffers.

There is a discrepancy in the data obtained at pH 1 between the HCl solution and the gastric solution (Fig. 1B). The fact that the pH was measured using pH test paper and we cannot know the value precisely might explain the discrepancy, especially at the extremely low pH.

The present study has shown that IFNAR plays an important role in the infection and multiplication of orally administered PV in the small intestine of hPVR-Tg (Fig. 4 and 5A). The deletion of IFNAR resulted in successful infection by oral PV via the intestinal epithelium and the subsequent development of clinical symptoms. Viremia seems to be essential for the symptoms to appear (Fig. 5B), and a histopathology for similar symptoms caused by artificial viremia (intravenous inoculation) in hPVR-Tg/*Ifnar*KO has been reported (13). We thus established an oral administration system using hPVR-Tg/*Ifnar*KO, with which one can assess the 100% lethal doses of PV strains. This is the first in vivo system in which all the animals showed paralysis after oral administration of PV.

From the results presented in Fig. 5B, the orally administered virus disseminates mainly through the bloodstream in mice, although other, minor routes might be involved. It is possible, for example, that a neural pathway exists from the alimentary tract to the CNS through the vagus nerve or from the skeletal muscle to the CNS through the peripheral nerve. After PVRTg21/*Ifnar*KO were orally administered 3×10^8 PFU of Sabin 1, low titers (from 4×10^1 PFU/plasma to 8×10^2 PFU/plasma) of virus were detected in the plasma for 2 of 3 mice 3 days after administration and for 1 of 3 mice 4 days after administration. In spite of the ineffective serum conversion (Table 1), some lethal infection occurs after oral administration of Sabin 1 in PVRTg21/*Ifnar*KO (Fig. 4C). These results imply that the neural pathway from the alimentary tract to the CNS might contribute to death after oral administration of Sabin 1 in PVRTg21/*Ifnar*KO. After oral administration, the titer of virus in skeletal muscle did not rise until the virus started replicating efficiently in all the tissues examined (data not shown). This result implies that the neural pathway from skeletal muscle to the CNS is not essential, at least in this system. Nevertheless, we do not know which pathway has an essential role in causing paralysis and death.

It is possible that the virus was incorporated accidentally via the intranasal pathway after oral administration. In our experiments, when 1.5×10^8 PFU/ml of the Mahoney strain was orally administered to PVRTg21, the mice showed hardly any signs of paralysis. This concentration was higher than 10^6 PFU/20 μl, which was enough to cause death among 60% of intranasally inoculated PVRTg21 (29). Furthermore, the distribution of the virus after oral administration differs from that after intranasal inoculation. From these results, it is unlikely that orally administered virus enters the intranasal pathway.

We have shown previously that hPVR is expressed in the small intestines of MPVRTg25 but is not detected in those of PVRTg21 by Western blotting (43). As for immunohistochemistry, hPVR expression was barely observed in the intestinal epithelium and was not detected in germinal centers within Peyer's patches in PVRTg21 (14), and an assertive hPVR antigen was not detected in small intestinal epithelia in PVRTg21 or MPVRTg25 (M. Takano-Maruyama and H. Ohno, personal communication). These results suggest that hPVR is not expressed at high levels in the small intestines of PVRTg21, MPVRTg25, or the *Ifnar* knockout versions of these mice, although it is possible that the levels of hPVR expression on the intestinal epithelia differ among these mice. Incorporated fluorescently labeled virus was observed in the intestines of MPVRTg25/*Ifnar*KO but not PVRTg21/*Ifnar*KO or C57BL/6 mice (data not shown). This might be due to the level of hPVR expression on the apical side of the intestinal epithelia. Despite the fact that PVRTg21 express little if any hPVR in the small intestine, the titers of virus in the upper small intestines of PVRTg21 and PVRTg21/*Ifnar*KO 1 day after administration were ~10^2-fold higher than those in C57BL/6 mice and C57BL/6/*Ifnar*KO, respectively (Fig. 5A), and PVRTg21/*Ifnar*KO showed susceptibility to oral administration of PV (Fig. 4A and C and 5). These results suggest that hPVR ex-

pressed in the small intestines of PVRTg21/*Ifnar*KO contributes to cell susceptibility to orally administered PV.

We observed hepatocirrhosis in MPVRTg25/*Ifnar*KO after oral administration of PV1(M)OM despite the fact that MPVRTg25 do not show hepatocirrhosis. These results suggest that MPVRTg25/*Ifnar*KO show irregular tissue tropism of the virus compared to MPVRTg25, which have a native immune system. A previous paper has reported that viral antigen-positive cells were detected in the liver 1 day after intravenous inoculation of 2×10^7 PFU of PV1(M)OM into MPVRTg25/*Ifnar*KO (13). Moreover, a high titer of the virus was recovered 2 days after oral administration of 3×10^8 PFU of PV1(M)OM to MPVRTg25/*Ifnar*KO (data not shown). It seems that this occurred because hPVR in the liver causes the virus to replicate in MPVRTg25/*Ifnar*KO mice. Indeed, we have reported previously that the liver in MPVRTg25 expresses hPVR (43). Moreover, the virus in the bloodstream can easily access the liver (1). Considering these results, it is feasible that the viremia led to a liver infection that then caused a secondary viremia, leading to invasion of the CNS in MPVRTg25/*Ifnar*KO. As for PVRTg21/*Ifnar*KO, it has been reported that the disruption of IFNAR enables the virus to replicate in nonneuronal tissues, although both PVRTg21 and PVRTg21/*Ifnar*KO developed paralysis by similar points in time after intravenous inoculation (13). All together, the oral infection system using hPVR-Tg/*Ifnar*KO does not serve as an adequate animal model for analyzing virus tissue tropism in the whole body, although the clinical symptoms seen in PVRTg21/*Ifnar*KO were similar to those in PVRTg21. This notion is also supported by the fact that healthy humans are highly susceptible to poliovirus infection in spite of a robust innate immune response. Nevertheless, this oral administration system might be applicable to the study of initial infection events in vivo. It is also worth elucidating the role of the IFNAR-related signaling cascade in the infection of intestinal epithelial cells.

We succeeded in detecting the fluorescently labeled virus in the small intestine 1 h after its injection (Fig. 6) but failed to detect the viral antigen 2 days after oral administration of the virus using immunohistochemistry (data not shown). It is difficult to detect antigens in the intestine because of high background levels and the quick turnover of infected cells. It is possible that the virus does not replicate prominently in the intestinal epithelia or that the infected cells tend to drop out easily from the epithelial layer. Although the titers of virus in other alimentary tissues were relatively low after oral administration of the virus (Fig. 5A) and the viral antigen was not detected in the NALT, esophagus, or colon 2 days after oral administration (data not shown), we cannot exclude the possibility that PV replicates in the alimentary tract early in the course of infection. Alternatively, the fluorescence observed could have derived from inactive PV taken up by cells during a nonproductive infection.

The mechanism for oral infection with PV in humans has not been made clear, though it is possible that PV can replicate in and/or permeate M cells or lymphatic tissues in humans, because attenuated PV vaccine strains can readily generate neutralizing antibodies. In the present study, oral administration of Sabin 1 did not lead to the generation of neutralizing activity in the serum of PVRTg21/*Ifnar*KO (Table 1) and MPVRTg25/*Ifnar*KO (data not shown) or the binding activity of immunoglobulin A's in feces (data not shown), despite the fact that the virus proliferated in the upper small intestine (data not shown). Our results also showed that PV was not preferentially detected in the UEA-1 fraction of epithelial cells, which contains M cells, in hPVR-Tg/*Ifnar*KO (Fig. 6C), and the virus did not proliferate efficiently in NALT, a lymphatic tissue (Fig. 5Ae and Be). These results may correlate with the difficulty of raising the neutralizing activity after oral administration of the virus in hPVR-Tg/*Ifnar*KO. However, it should be emphasized that a lack of IFNAR hampered enhancement of the antibody-evoked response (23). Thus, the phenomena we observed might be due to the lack of IFNAR. Although we still could not reconcile the discrepancy between humans and the murine model in the exact site of PV invasion in the intestinal tract, the present study offers a new opportunity to address the issue, since hPVR-Tg/*Ifnar*KO are susceptible to orally administered PV for the initiation of infection and subsequent development of disease symptoms. And it is probable that the expression of hPVR in different intestinal cells is important in determining the heightened permissiveness of oral PV administration in humans compared to rodents. PV is highly successful at infection of the alimentary tracts of humans, and intestinal secretion of the virus can persist for months, even in healthy individuals, regardless of age. This means that the virus infects and replicates in some cells or tissues in the human gastrointestinal tract in spite of a possible early innate immune response. However, it is also possible that the innate immune response of humans is weaker than that of rodents.

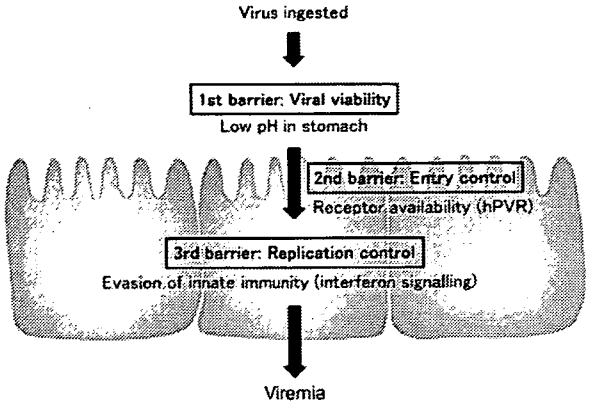

FIG. 7. Presumed PV dissemination routes and characteristics. The presumed barriers to orally ingested PV are shown. First, the ingested virus enters the stomach and suffers a low-pH environment (the first barrier). Second, the virus has to find the appropriate receptor in order to enter the intestinal cells (the second barrier, cell susceptibility). Third, the virus can start replicating in the cells depending on the lack of an IFN system (the third barrier, cell permissivity). Finally, the virus probably invades the bloodstream.

The presumed barriers to orally ingested PV are shown in Fig. 7. First, the ingested virus enters the stomach and experiences a low-pH environment (the first barrier). If the virus overcomes this, it has to find the appropriate receptor in order to enter the intestinal cells (the second barrier, cell susceptibility). Then the virus can start replicating in the cells depending on the lack of an IFN system (the third barrier, cell permissivity). Finally, the virus probably invades the bloodstream. In this report, we clarified that the low pH of the gastric

environment inactivates PV and decreases the titer of virus that reaches the intestine, and the lack of an IFN system allows the virus to replicate in the intestine more efficiently. These three barriers may serve to protect individuals from viremia.

ACKNOWLEDGMENTS

We are grateful to T. Matano for suggestions and discussions. We also thank A. Ohmura for help in breeding the mice and E. Suzuki for help in preparing the manuscript.

This work was supported in part by Grants-in-Aid for Advanced Medical Science Research, a Grant-in-Aid for Scientific Research on Priority Areas by the Ministry of Education, Culture, Sports, Science and Technology, Japan, and a grant from the Ministry of Health and Welfare of Japan.

REFERENCES

1. **Aoki, J.** 1994. Tissue tropism and species specificity of poliovirus infection. Tanpakushitsu Kakusan Koso **39:**2081–2089.
2. **Bodian, D.** 1955. Emerging concept of poliomyelitis infection. Science **122:** 105–108.
3. **Chebath, J., P. Benech, M. Revel, and M. Vigneron.** 1987. Constitutive expression of (2′–5′) oligo A synthetase confers resistance to picornavirus infection. Nature **330:**587–588.
4. **Clark, M. A., M. A. Jepson, N. L. Simmons, T. A. Booth, and B. H. Hirst.** 1993. Differential expression of lectin-binding sites defines mouse intestinal M-cells. J. Histochem. Cytochem. **41:**1679–1687.
5. **Coccia, E. M., G. Romeo, A. Nissim, G. Marziali, R. Albertini, E. Affabris, A. Battistini, G. Fiorucci, R. Orsatti, G. B. Rossi, et al.** 1990. A full-length murine 2-5A synthetase cDNA transfected in NIH-3T3 cells impairs EMCV but not VSV replication. Virology **179:**228–233.
6. **Fiette, L., C. Aubert, U. Muller, S. Huang, M. Aguet, M. Brahic, and J. F. Bureau.** 1995. Theiler's virus infection of 129Sv mice that lack the interferon alpha/beta or interferon gamma receptors. J. Exp. Med. **181:**2069–2076.
7. **Flint, S. J., R. M. Enquist, V. R. Racaniello, and A. M. Skalka.** 2003. Principles of virology: molecular biology, pathogenesis, and control of animal viruses. ASM Press, Washington, DC.
8. **Garcia-Sastre, A., R. K. Durbin, H. Zheng, P. Palese, R. Gertner, D. E. Levy, and J. E. Durbin.** 1998. The role of interferon in influenza virus tissue tropism. J. Virol. **72:**8550–8558.
9. **Gromeier, M., and E. Wimmer.** 1998. Mechanism of injury-provoked poliomyelitis. J. Virol. **72:**5056–5060.
10. **Horie, H., S. Koike, T. Kurata, Y. Sato-Yoshida, I. Ise, Y. Ota, S. Abe, K. Hioki, H. Kato, C. Taya, T. Nomura, S. Hashizume, H. Yonekawa, and A. Nomoto.** 1994. Transgenic mice carrying the human poliovirus receptor: new animal models for study of poliovirus neurovirulence. J. Virol. **68:**681–688.
11. **Howe, H., and D. Bodian.** 1942. Neuronal mechanisms in poliomyelitis. Commonwealth Fund, New York, NY; Humphrey Milford, Oxford University Press, London, England.
12. **Hsiung, G. D., F. L. Black, and J. R. Henderson.** 1964. Susceptibility of primates to viruses in relation to taxonomic classification, p. 1–23. *In* J. Buettner-Janusch (ed.), Evolutionary and genetic biology of primates, vol. II. Academic Press, New York, NY.
13. **Ida-Hosonuma, M., T. Iwasaki, T. Yoshikawa, N. Nagata, Y. Sato, T. Sata, M. Yoneyama, T. Fujita, C. Taya, H. Yonekawa, and S. Koike.** 2005. The alpha/beta interferon response controls tissue tropism and pathogenicity of poliovirus. J. Virol. **79:**4460–4469.
14. **Iwasaki, A., R. Welker, S. Mueller, M. Linehan, A. Nomoto, and E. Wimmer.** 2002. Immunofluorescence analysis of poliovirus receptor expression in Peyer's patches of humans, primates, and CD155 transgenic mice: implications for poliovirus infection. J. Infect. Dis. **186:**585–592.
15. **Jang, M. H., M. N. Kweon, K. Iwatani, M. Yamamoto, K. Terahara, C. Sasakawa, T. Suzuki, T. Nochi, Y. Yokota, P. D. Rennert, T. Hiroi, H. Tamagawa, H. Iijima, J. Kunisawa, Y. Yuki, and H. Kiyono.** 2004. Intestinal villous M cells: an antigen entry site in the mucosal epithelium. Proc. Natl. Acad. Sci. USA **101:**6110–6115.
16. **Kajigaya, S., H. Arakawa, S. Kuge, T. Koi, N. Imura, and A. Nomoto.** 1985. Isolation and characterization of defective-interfering particles of poliovirus Sabin 1 strain. Virology **142:**307–316.
17. **Kandori, H., K. Hirayama, M. Takeda, and K. Doi.** 1996. Histochemical, lectin-histochemical and morphometrical characteristics of intestinal goblet cells of germfree and conventional mice. Exp. Anim. **45:**155–160.
18. **Kew, O. M., R. W. Sutter, E. M. de Gourville, W. R. Dowdle, and M. A. Pallansch.** 2005. Vaccine-derived polioviruses and the endgame strategy for global polio eradication. Annu. Rev. Microbiol. **59:**587–635.
19. **Kohara, M., S. Abe, T. Komatsu, K. Tago, M. Arita, and A. Nomoto.** 1988. A recombinant virus between the Sabin 1 and Sabin 3 vaccine strains of poliovirus as a possible candidate for a new type 3 poliovirus live vaccine strain. J. Virol. **62:**2828–2835.
20. **Koike, S., J. Aoki, and A. Nomoto.** 1994. Transgenic mice for the study of poliovirus pathogenicity, p. 463–480. *In* E. Wimmer and R. Weiss (ed.), Cellular receptors for animal viruses. Cold Spring Harbor Laboratory Press, Plainview, NY.
21. **Koike, S., C. Taya, J. Aoki, Y. Matsuda, I. Ise, H. Takeda, T. Matsuzaki, H. Amanuma, H. Yonekawa, and A. Nomoto.** 1994. Characterization of three different transgenic mouse lines that carry human poliovirus receptor gene—influence of the transgene expression on pathogenesis. Arch. Virol. **139:**351–363.
22. **Koike, S., C. Taya, T. Kurata, S. Abe, I. Ise, H. Yonekawa, and A. Nomoto.** 1991. Transgenic mice susceptible to poliovirus. Proc. Natl. Acad. Sci. USA **88:**951–955.
23. **Le Bon, A., G. Schiavoni, G. D'Agostino, I. Gresser, F. Belardelli, and D. F. Tough.** 2001. Type I interferons potently enhance humoral immunity and can promote isotype switching by stimulating dendritic cells in vivo. Immunity **14:**461–470.
24. **Meurs, E. F., Y. Watanabe, S. Kadereit, G. N. Barber, M. G. Katze, K. Chong, B. R. Williams, and A. G. Hovanessian.** 1992. Constitutive expression of human double-stranded RNA-activated p68 kinase in murine cells mediates phosphorylation of eukaryotic initiation factor 2 and partial resistance to encephalomyocarditis virus growth. J. Virol. **66:**5805–5814.
25. **Morrison, M. E., and V. R. Racaniello.** 1992. Molecular cloning and expression of a murine homolog of the human poliovirus receptor gene. J. Virol. **66:**2807–2813.
26. **Mrkic, B., J. Pavlovic, T. Rulicke, P. Volpe, C. J. Buchholz, D. Hourcade, J. P. Atkinson, A. Aguzzi, and R. Cattaneo.** 1998. Measles virus spread and pathogenesis in genetically modified mice. J. Virol. **72:**7420–7427.
27. **Muller, U., U. Steinhoff, L. F. Reis, S. Hemmi, J. Pavlovic, R. M. Zinkernagel, and M. Aguet.** 1994. Functional role of type I and type II interferons in antiviral defense. Science **264:**1918–1921.
28. **Munoz, A., and L. Carrasco.** 1984. Action of human lymphoblastoid interferon on HeLa cells infected with RNA-containing animal viruses. J. Gen. Virol. **65:**377–390.
29. **Nagata, N., T. Iwasaki, Y. Ami, Y. Sato, I. Hatano, A. Harashima, Y. Suzaki, T. Yoshii, T. Hashikawa, T. Sata, Y. Horiuchi, S. Koike, T. Kurata, and A. Nomoto.** 2004. A poliomyelitis model through mucosal infection in transgenic mice bearing human poliovirus receptor, TgPVR21. Virology **321:**87–100.
30. **Nathanson, N., and A. D. Langmuir.** 1963. The Cutter incident. Poliomyelitis following formaldehyde-inactivated poliovirus vaccination in the United States during the spring of 1955. III. Comparison of the clinical character of vaccinated and contact cases occurring after use of high rate lots of Cutter vaccine. Am. J. Hyg. **78:**61–81.
31. **Ohka, S., W. X. Yang, E. Terada, K. Iwasaki, and A. Nomoto.** 1998. Retrograde transport of intact poliovirus through the axon via the fast transport system. Virology **250:**67–75.
32. **Pelkmans, L., J. Kartenbeck, and A. Helenius.** 2001. Caveolar endocytosis of simian virus 40 reveals a new two-step vesicular-transport pathway to the ER. Nat. Cell Biol. **3:**473–483.
33. **Ren, R., and V. R. Racaniello.** 1992. Human poliovirus receptor gene expression and poliovirus tissue tropism in transgenic mice. J. Virol. **66:**296–304.
34. **Ren, R., and V. R. Racaniello.** 1992. Poliovirus spreads from muscle to the central nervous system by neural pathways. J. Infect. Dis. **166:**747–752.
35. **Ren, R. B., F. Costantini, E. J. Gorgacz, J. J. Lee, and V. R. Racaniello.** 1990. Transgenic mice expressing a human poliovirus receptor: a new model for poliomyelitis. Cell **63:**353–362.
36. **Ryman, K. D., W. B. Klimstra, K. B. Nguyen, C. A. Biron, and R. E. Johnston.** 2000. Alpha/beta interferon protects adult mice from fatal Sindbis virus infection and is an important determinant of cell and tissue tropism. J. Virol. **74:**3366–3378.
37. **Sabin, A. B.** 1965. Oral poliovirus vaccine: history of its development and prospects for eradication of poliomyelitis. JAMA **194:**872–876.
38. **Sabin, A. B.** 1956. Pathogenesis of poliomyelitis: reappraisal in the light of new data. Science **123:**1151–1157.
39. **Sabin, A. B., and L. R. Boulger.** 1973. History of Sabin attenuated poliovirus oral live vaccine strains. J. Biol. Stand. **1:**115–118.
40. **Salo, R. J., and D. O. Cliver.** 1976. Effect of acid pH, salts, and temperature on the infectivity and physical integrity of enteroviruses. Arch. Virol. **52:**269–282.
41. **Shiroki, K., T. Ishii, T. Aoki, M. Kobashi, S. Ohka, and A. Nomoto.** 1995. A new *cis*-acting element for RNA replication within the 5′ noncoding region of poliovirus type 1 RNA. J. Virol. **69:**6825–6832.
42. **Wessely, R., K. Klingel, K. U. Knowlton, and R. Kandolf.** 2001. Cardioselective infection with coxsackievirus B3 requires intact type I interferon signaling: implications for mortality and early viral replication. Circulation **103:**756–761.
43. **Yanagiya, A., S. Ohka, N. Hashida, M. Okamura, C. Taya, N. Kamoshita, K. Iwasaki, Y. Sasaki, H. Yonekawa, and A. Nomoto.** 2003. Tissue-specific

replicating capacity of a chimeric poliovirus that carries the internal ribosome entry site of hepatitis C virus in a new mouse model transgenic for the human poliovirus receptor. J. Virol. **77**:10479–10487.

44. **Yang, W. X., T. Terasaki, K. Shiroki, S. Ohka, J. Aoki, S. Tanabe, T. Nomura, E. Terada, Y. Sugiyama, and A. Nomoto.** 1997. Efficient delivery of circulating poliovirus to the central nervous system independently of poliovirus receptor. Virology **229**:421–428.
45. **Zhang, S., and V. R. Racaniello.** 1997. Expression of the poliovirus receptor in intestinal epithelial cells is not sufficient to permit poliovirus replication in the mouse gut. J. Virol. **71**:4915–4920.
46. **Zhou, A., J. Paranjape, T. L. Brown, H. Nie, S. Naik, B. Dong, A. Chang, B. Trapp, R. Fairchild, C. Colmenares, and R. H. Silverman.** 1997. Interferon action and apoptosis are defective in mice devoid of 2′,5′-oligoadenylate-dependent RNase L. EMBO J. **16**:6355–6363.

Review

Molecular aspects of poliovirus pathogenesis

By Akio NOMOTO[*1,*2,†]

(Communicated by Kumao TOYOSHIMA, M.J.A.)

Abstract: The development of a transgenic mouse model carrying the human poliovirus receptor has made it possible to investigate the molecular mechanisms of the viral dissemination process in a whole organism. Studies on this have provided an insight into the mechanisms for viral permeation through the blood-brain barrier and retrograde axonal transport of the virus. In addition, strain-specific neurovirulence levels are shown to depend mainly on the replicating capacity of the virus in the central nervous system rather than the efficiency of the 2 dissemination pathways indicated above. Studies of poliovirus-induced cytopathic effects on neural cells revealed that neural cells possess anti-poliovirus characteristics that may offer a new avenue for investigating the molecular mechanisms of poliovirus neurovirulence.

Keywords: poliovirus, transgenic mouse, poliovirus receptor, dissemination, neurovirulence

Introduction

Poliovirus, a human enterovirus that belongs to the family Picornaviridae, is the causative agent of poliomyelitis. Humans are the only natural hosts of poliovirus. The virus, however, can be transferred to monkeys when it is directly inoculated into the central nervous system (CNS). The species specificity of this virus is governed by a specific cell surface molecule that serves as the poliovirus receptor (PVR).[1),2)] Indeed, transgenic mice carrying the human poliovirus receptor (hPVR/CD155) gene show susceptibility to poliovirus infection, although mice in general are not susceptible to poliovirus.[3),4)]

In humans, poliovirus infection usually begins with oral ingestion of the virus. After oral ingestion, the virus multiplies in the alimentary mucosa, and possibly in the tonsils and Peyer's patches. The virus then moves into the blood stream (viremia) through the putative barrier(s) that virulent poliovirus strains cross more efficiently than attenuated strains. The circulating virus invades the CNS and replicates in neurons, particularly motor neurons. There are 2 possible dissemination routes through which the circulating poliovirus can enter the CNS. One is virus permeation through the blood-brain barrier (BBB), and the other is virus transmission via peripheral nerves (Fig. 1). Paralytic poliomyelitis occurs as a result of neuronal destruction by lytic replication of the poliovirus, although paralysis develops in less than 1% of those infected.[5),6)]

A poliovirion consists of a single-stranded RNA genome of positive polarity and a non-enveloped capsid that comprises 60 copies of each of 4 capsid proteins: VP1, VP2, VP3, and VP4. The three-dimensional structure has been elucidated,[7)] and the study revealed depressions called "canyons" on the virion surface, which have been shown to be attachment sites for PVR.[8)–10)] The genome of the poliovirus functions as mRNA in the cytoplasm of infected cells. The virus-specific translation process begins with the entry of ribosomes into the internal ribosome entry site (IRES) within the 5′ noncoding sequence of the RNA,[11)] and all viral proteins are translated as a large precursor protein from a single

*1 Department of Microbiology, Graduate School of Medicine, The University of Tokyo, Tokyo, Japan.
*2 Recipient of the Japan Academy Prize in 2004.
† Department of Microbiology, Graduate School of Medicine, The University of Tokyo, 7-3-1 Hongo, Bunkyo-ku, Tokyo 113-0033, Japan (e-mail: anomoto@m.u-tokyo.ac.jp).

Abbreviations: PVR: poliovirus receptor; hPVR: human poliovirus receptor; CNS: central nervous system; IRES: internal ribosome entry site; OPV: oral poliovaccine; BBB: blood-brain barrier; mAb: monoclonal antibody; hpi: hours post infection.

doi: 10.2183/pjab/83.266

open reading frame that is cotranslationally processed into functional viral proteins (Fig. 2).

Poliovirus is classified into 3 stable serotypes (types 1, 2, and 3), and each serotype can cause poliomyelitis. To control poliomyelitis, attenuated poliovirus strains of all 3 serotypes (Sabin 1, Sabin 2, and Sabin 3) have been developed and used effectively as oral poliovaccines (OPV).[12] After oral administration, these Sabin strains can replicate to a sufficiently high level in the human alimentary tract to elicit neutralizing antibodies, although the virus has little capacity to move into the blood stream and replicate in the CNS.

The result of viral dissemination studies using polio-sensitive transgenic mice is reviewed here. In addition, the anti-poliovirus response indicated by poliovirus-infected neural cells is described as a new aspect of poliovirus neurovirulence.

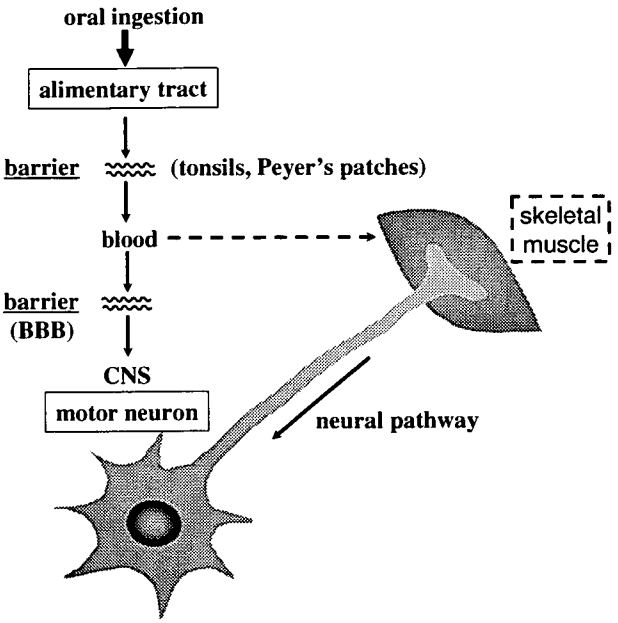

Fig. 1. Dissemination pathways of poliovirus in humans.

A mouse model for poliomyelitis

The hPVR (CD155) is a member of the immunoglobulin (Ig) superfamily, with 3 linked extracellular Ig-like domains followed by a membrane-spanning domain and a cytoplasmic domain[1),2)] (Fig. 3). Molecular genetic analysis revealed that the amino-terminal Ig-like domain is essential for poliovirus binding and infection.[13)–16)] Currently, 4 mRNA isoforms are known to be generated by alternative splicing[2)] and translated into 4 different forms of hPVRs, namely, hPVRα, hPVRβ, hPVRγ, and hPVRδ (Fig. 4). Of these, hPVRβ and hPVRγ lack the transmembrane domain and therefore soluble forms. Two other hPVRs, namely, hPVRα and hPVRδ are functional poliovirus receptors. They differ only in a region of the amino-acid sequence of their carboxyl-termini of the cytoplasmic domain (Fig. 5). Although hPVR is reported to bind CD226, a cell surface molecule of NK cells, and activate NK cells,[17),18)] it is not known whether activation of NK cells is the

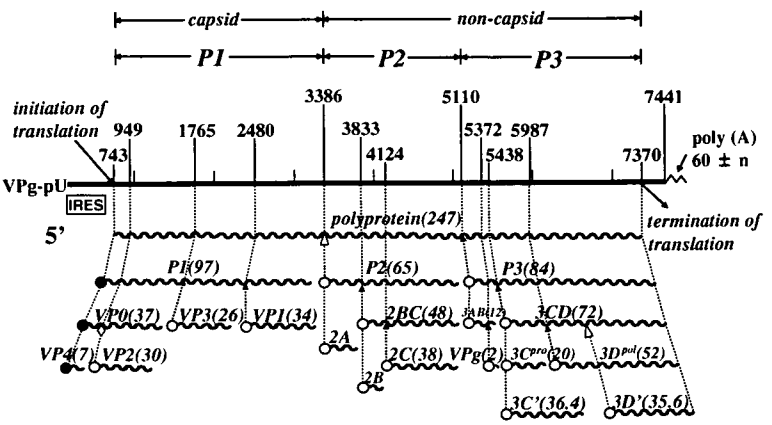

Fig. 2. Genome organization of poliovirus type 1. Genomic RNA and its gene organization are shown. VPg is a small protein attached to the 5′ end of the genome; poly(A) is 3′ terminal. Nucleotide numbers are shown over the genome RNA. P1 represents the protein region of viral capsid; P2 and P3 non-capsid protein. Gene products are indicated by wavy lines, and figures in parentheses are molecular mass of the corresponding viral gene products. IRES stands for internal ribosome entry site.

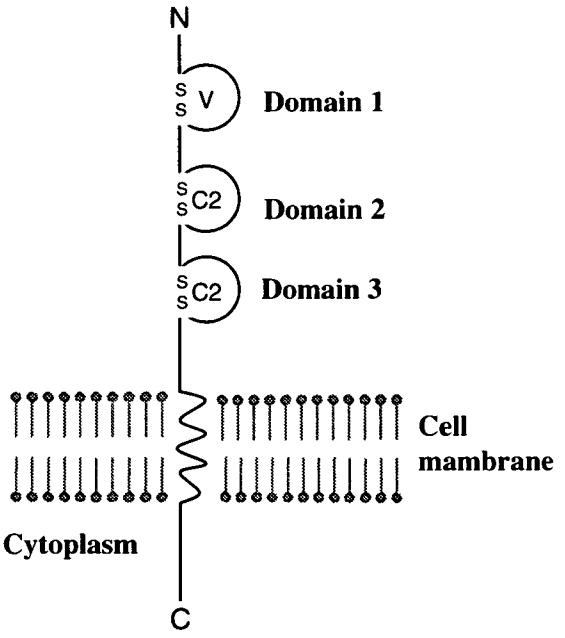

Fig. 3. Schematic structure of human poliovirus receptor α (hPVRα). Three linked extracellular Ig-like domains (V, C2, and C2 types) are followed by a membrane-spanning domain and a cytoplasmic domain.

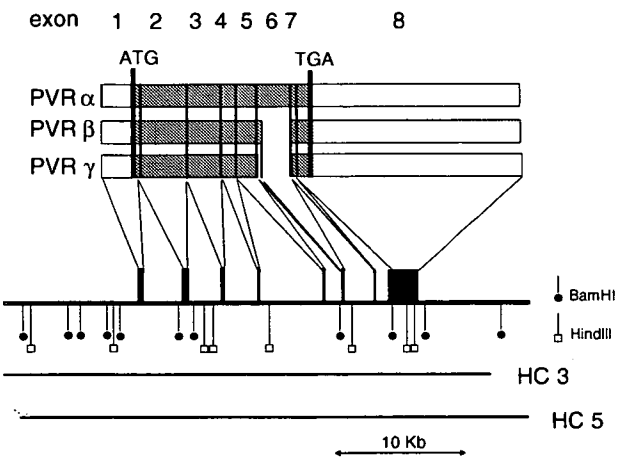

Fig. 4. Restriction map of the human PVR gene and multiple splicing of its transcript. Structures of mRNAs for hPVRα, hPVRβ, and hPVRγ are shown by open (untranslated sequences) and shaded (translated sequences) boxes. Numbers of exons are indicated at the top of the figure. Receptor regions are connected by thin lines to exons contained on a gene map shown underneath. Restriction cleavage sites of *Bam*HI and *Hin*dIII are indicated by vertical bars with closed circles and open boxes, respectively. Sequences of the human PVR gene cloned into cosmids HC3 and HC5 are indicated by bars. A scale for length of nucleotides of the PVR gene is shown by bar with arrowheads at both ends at the bottom of the figure. (quoted from ref. 2).

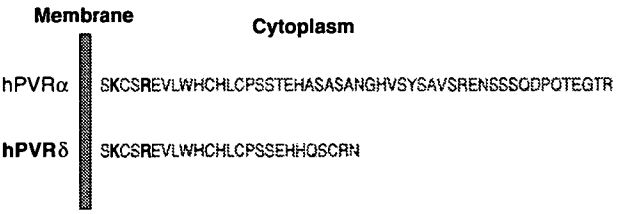

Fig. 5. Amino acid sequences of cytoplasmic domains of hPVRα and hPVRδ.

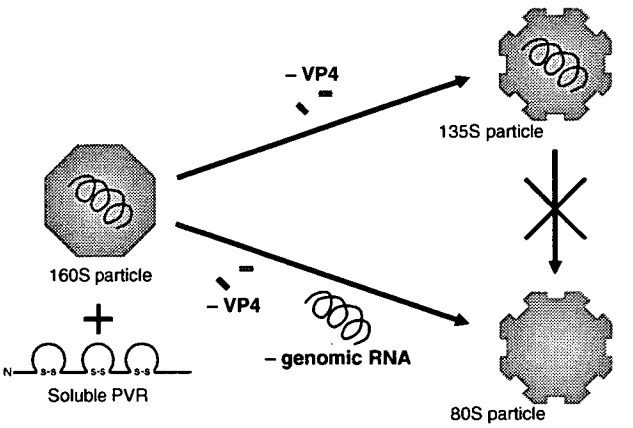

Fig. 6. Conformational alteration of 160S (intact) poliovirus particle induced by the addition of soluble hPVR. Infectious poliovirus (160S) converts to 135S and 80S particles when the virus (160S) is incubated with the extracellular domain of hPVR *in vitro*.

only physiological function of the hPVRs and why 4 different forms of hPVRs are generated.

Poliovirus alters its conformation when hPVR binds the virus, and hPVR is thought to be the only molecule that is involved in the uncoating process of poliovirus. Indeed, infectious poliovirus (160S) converts to 135S and 80S particles when the virus (160S) is incubated with the extracellular domain of hPVR *in vitro*.[19),20)] A 135S particle has lost the internal protein VP4, and an 80S particle, the RNA genome as well as VP4 (Fig. 6). It is indicated that poliovirus uncoating proceeds independently of an acidic pH environment in cultured cells.[19)–21)]

A transgenic (Tg) mouse carrying the hPVR gene (PVR-Tg mouse) showed susceptibility to poliovirus by intravenous (IV), intramuscular (IM), intracerebral (IC), or intraspinal (ISp) inoculation.[3),4),22)–26)] Transgenic mice infected via any of these 4 inoculation routes show signs of paralysis that resemble those of poliomyelitis in humans

and monkeys. The results of histocytochemical examinations of the CNS of paralyzed mice are also similar to those of humans and monkeys.[4),24)] Furthermore, mouse neurovirulence levels of individual poliovirus strains using the PVR-Tg21 mouse model with an ISp or IC inoculation route are parallel with monkey neurovirulence.[23),24)] Based on these results, PVR-Tg21 mice, in addition to monkeys, are recognized by the World Health Organization (WHO) as an alternative poliomyelitis animal model. The susceptibility of PVR-Tg21 mice to orally administered poliovirus is, if any, very low (similar to that of monkeys), probably because of a strong response by interferon signaling in the gut of mice. This notion was recently proved by using PVR-Tg mice that are deficient in the type I interferon receptor.[27)] In addition, poliovirus was shown to be inactivated by the low pH of the gastric contents in mice.[27)]

The development of a mouse model for poliomyelitis makes it considerably simpler to investigate the efficiency of poliovirus dissemination in an entire organism. For example, the efficiencies of viral BBB permeation[25)] and retrograde axonal transport[26)] can be estimated after viral IV inoculation and viral IM inoculation, respectively. The results of these experiments performed using transgenic mice are described below.

Blood-brain barrier permeation

Physiological pharmacokinetic analysis was employed to investigate the fate of poliovirus inoculated into the tail vein of mice.[25)] The inoculated virus is distributed to various tissues, such as the spleen, liver, kidney, small intestine, heart, lung, muscle, and CNS tissues. The amount of poliovirus delivered to the CNS tissues, including the cerebellum and cerebrum, are the smallest. However, this amount is significantly greater than the theoretical amount estimated within the vascular volume of the brain. In contrast, the amount of poliovirus distributed to other tissues almost equals the theoretical amount predicted based on vascular volume. These data suggest that poliovirus passes through the BBB.

Unexpectedly, the distribution profiles of the virus 5 h after the inoculation to transgenic and non-transgenic mice are similar (Fig. 7). This suggests that specific distribution of poliovirus to the CNS tissues is not due to the expression of

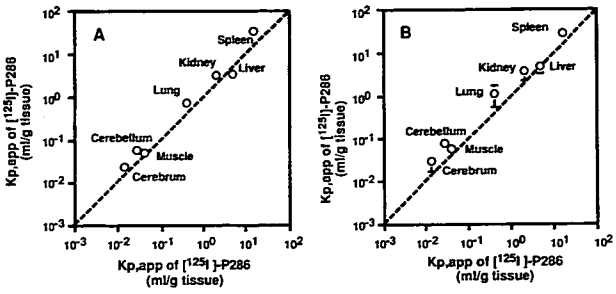

Fig. 7. Tissue distribution of poliovirus in mice after intravenous inoculation. (A) $K_{p,app}$ values of [^{35}S]methionine-labeled MSM (a recombinant poliovirus Mahoney strain having the Sabin 1 derived capsid proteins) in various tissues were calculated in transgenic mice (vertical axis) and non-transgenic mice (horizontal axis) 5 h after the IV inoculation. (B) Transgenic mice were IV-injected with mAb p286 5 h before the IV inoculation of [^{35}S]methionine-labeled MSM. $K_{p,app}$ values of MSM in various tissues were calculated (vertical axis) and transgenic mice pretreated with the mAb (horizontal axis) 5 h after the inoculation. (quoted from ref. 25).

Table 1. Rate of accumulation of poliovirus in the mouse cerebrum[a,b]

Control materials	Tg mouse	Non-Tg mouse	Rat
Virulent Mahoney	164	123	—
Attenuated Sabin 1	223	246	—
Albumin	—	1[c]	—
Cationized RSA	—	—	123

[a]Abbreviation: Tg, transgenic.
RSA, rat serum albumin.
[b]Modified from Ref 25.
[c]0.001 μl min^{-1} g^{-1} tissue is regarded as 1.

hPVR. This is supported by results of experiments in which the pre-administration of anti-hPVR monoclonal antibody (mAb) p286 did not affect the distribution profile of poliovirus in transgenic mice (Fig. 7). MAb p286 as well as mAb p403[16)] has an ability to block binding and infection of poliovirus to susceptible cells. These results indicate that hPVR expression in transgenic mice does not play a significant role in the tissue distribution profile of poliovirus until 5 h after IV inoculation.

The linear accumulation of poliovirus in the CNS tissues was observed at least 7.5 h after inoculation.[25)] The accumulation rates in the brains of transgenic and non-transgenic mice were compared for the virulent and attenuated strains of poliovirus type 1 and control materials (Table 1).

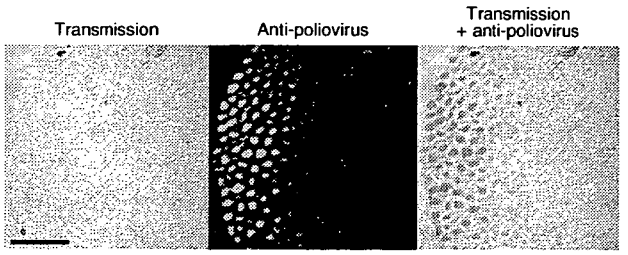

Fig. 8. Poliovirus antigens in axons. The sections of the sciatic nerves were prepared from a poliovirus-infected Tg mouse. The sections were immunostained with rabbit anti-poliovirus hyperimmune serum. (Left panel) Myelin sheaths can be seen. (Center panel) Bright fluorescence is visible. (Right panel) Merging picture of the left and center panels. Poliovirus antigens existing in axons surrounded by myelin sheath. Bar = 50 μm. (modified from ref. 26).

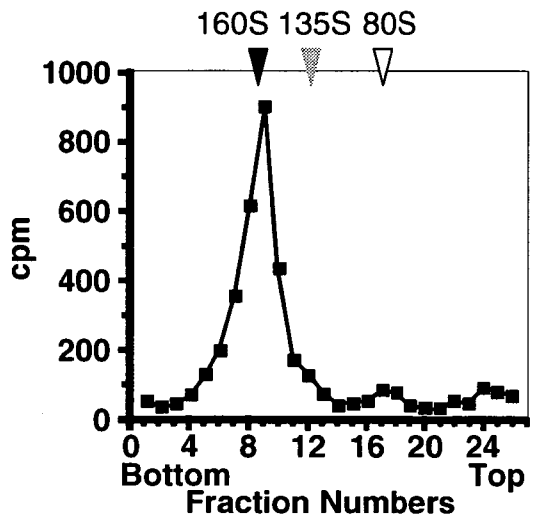

Fig. 9. Analysis of virus-related materials in the sciatic nerve. Tg mice with sciatic nerve ligation were intramuscularly inoculated with [^{35}S]methionine-labeled poliovirus Mahoney strain. Radioactive materials were recovered from the sciatic nerve and analyzed by sucrose density gradient centrifugation. (modified from ref. 26).

The difference in accumulation rates between the virulent Mahoney and attenuated Sabin 1 strains were not clearly significant. In addition, the accumulation rate observed in transgenic mice was similar to that in non-transgenic mice, supporting the notion that the hPVR does not play an important role in delivering circulating poliovirus to the tissues.

The rates of accumulation of the virus in the brain is more than 100 times higher than that of

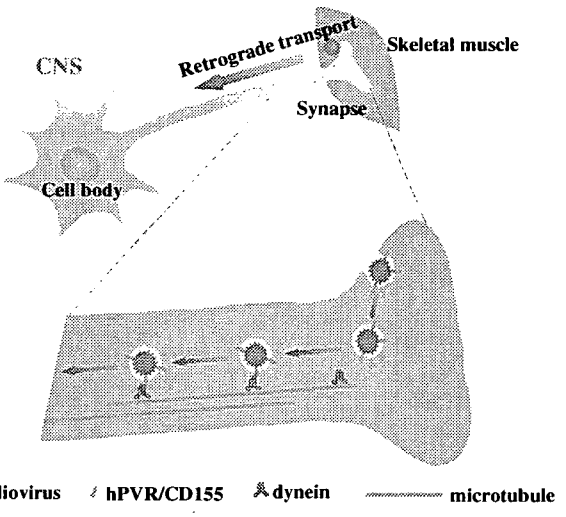

Fig. 10. Possible mechanism for the retrograde axonal transport of poliovirus.

albumin, which is not thought to permeate the BBB via a specific transport system, and is similar to that of cationized rat serum albumin, which is known to efficiently permeate the BBB (Table 1). These data suggest that polioviruses permeate the BBB at a fairly high degree of efficiency, independent of the hPVR or virus strains. Thus, some host cell molecules other than hPVR must be involved in the BBB permeation of poliovirus.

To elucidate mechanisms for the BBB permeation of poliovirus *in vitro*, an experimental system is required. We are currently investigating the BBB permeation mechanism of poliovirus by using mouse vascular endothelial cells cultured in a transwell.

Retrograde axonal transport

A pathway of the neural dissemination caused poliovirus has been reported for humans, monkeys, and transgenic mice. A high frequency of initial paralysis was observed in the inoculated limb in the Cutter vaccine incident, in which children received incompletely inactivated polio vaccine prepared from virulent poliovirus strains.[28] In addition, experimental evidence has indicated that poliovirus can spread to the CNS through the sciatic nerve of monkeys and transgenic mice.[29] Using transgenic mice, mouse neurovirulence induced by this dissemination route was shown to require hPVR. Furthermore, provocation poliomyelitis, a phenomenon resulting from physical trauma during polio-